



# Seismic hazard zonation map and definition of seismic actions for Greece in the context of the ongoing revision of EC8

Kyriazis Pitilakis<sup>1</sup> · Evi Riga<sup>1</sup> · Stefania Apostolaki<sup>1</sup> · Laurentiu Danciu<sup>2</sup>

Received: 28 August 2023 / Accepted: 8 April 2024  
© The Author(s) 2024

## Abstract

The Greek National Annex for current Eurocode 8 has adopted the seismic hazard zonation map published in 2003 as part of the modifications to the Greek Seismic Code EAK 2000 (EAK 2003). This map, which followed the catastrophic earthquakes that hit the country between 1978 and 2001, includes three seismic hazard zones with peak ground acceleration (PGA) ranging between 0.16 and 0.36 g. In this paper, following the significant progress that has been made worldwide in the last two decades towards the improvement of the definition of seismic actions and the seismic hazard maps using fully probabilistic models, we make a complete proposal for the Greek National Annex of the ongoing revision of Eurocode 8, which includes a new seismic hazard zonation map for Greece, as well as a novel site categorization scheme and related site amplification factors. To this end, we use the results of the European Seismic Hazard Model, ESHM20, as reported by Danciu et al. (The 2020 update of the European Seismic Hazard Model: Model Overview, 2021) which will be adopted as informative reference for the seismic hazard at European level in the forthcoming revision of Eurocode 8 (CEN/EC8). The herein proposed ground shaking zonation for rock conditions includes five zones with PGA values ranging between 0.13 and 0.37 g. For each zone, two newly proposed ground motion parameters, i.e.,  $S_{\alpha,475}$  and  $S_{\beta,475}$ , are provided, which are the two parameters used for anchoring the elastic response spectrum as defined in CEN/EC8, along with all the other necessary parameters for the definition of the elastic response spectrum, including site amplification. The proposal for the new seismic zonation is supported by a preliminary investigation of the impact of its adoption on the seismic design of new structures and on the seismic risk of the current building stock in Greece, to help gain a better insight on how important the differences imposed by the new zonation might be for the end-users and the administration.

**Keywords** Eurocode 8 · Greece · Seismic hazard map · ESHM20 · Site amplification · Elastic response spectra · Seismic risk

---

✉ Evi Riga  
eviriga@civil.auth.gr

<sup>1</sup> Aristotle University of Thessaloniki, P.O.B. 424, 54124 Thessaloniki, Greece

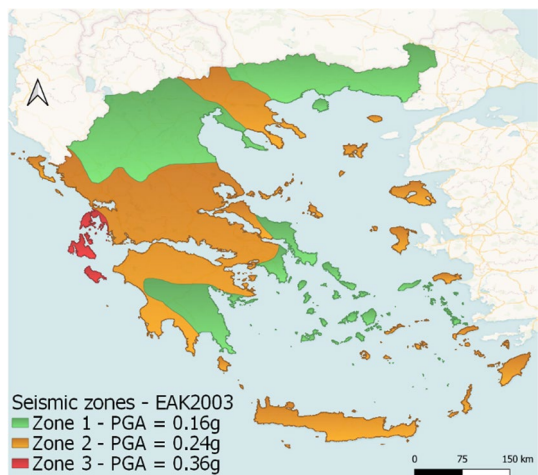
<sup>2</sup> Swiss Seismological Service (SED), ETH, Sonneggstrasse 5, 8092 Zurich, Switzerland

## 1 Introduction

Greece is the most seismically active region in Europe, and therefore the European country with the highest seismic hazard. The current seismic hazard zonation map for Greece, in force since 2003, is essentially an update of the zonation of the 1992 seismic code NEAK and came as a consequence of the many catastrophic earthquakes that hit Greece between 1978 and 2001 (e.g. M 6.4 Thessaloniki event in 1978, M 6.2 Kalamata in 1986, M 6.6 Kozani-Grevena and M 6.4 Aigio events in 1995, M 5.9 Athens event in 1999). This map was prepared jointly by the main seismological research centres of Greece (University of Athens, Aristotle University of Thessaloniki, Geodynamic Institute of the National Observatory of Athens, Institute of Engineering Seismology and Earthquake Engineering and University of Patras) and includes three seismic hazard zones with peak ground acceleration values, PGA, of 0.16, 0.24 and 0.36 g (Fig. 1). No site-specific amplification factors were proposed in that version of the code.

In the last two decades, a lot of efforts have been made to improve the seismic hazard maps worldwide, adopting the results of probabilistic seismic hazard analyses. In Italy, a new probabilistic seismic hazard model, MPS19, was developed in 2019 by the Seismic Hazard Center of the Istituto Nazionale di Geofisica e Vulcanologia (INGV), taking into account a large amount of recent data and methods (Meletti et al. 2021). In Turkey, updated probabilistic seismic hazard maps were developed with the support of the Disaster and Emergency Management Authority of Turkey (AFAD) (Akkar et al., 2007), in line with the development of the new seismic design code. In USA, the national seismic hazard model was updated in 2017–2018 with the incorporation of an updated seismicity catalogue, new ground motion models, and basin terms for long periods (Petersen et al. 2020). In New Zealand, a revision of the probabilistic National Seismic Hazard Model was released in 2022, including revised seismic hazard maps, hazard curves and Uniform Hazard Spectra, disaggregation results as well as a web tool to make the results of the model openly available. Regarding similar efforts at European level, the European Seismic Hazard Model ESHM20 (Danciu et al. 2021) was publicly released in April 2022. ESHM20 was developed within the framework of the EU-funded project “Seismology and Earthquake Engineering Research Infrastructure Alliance for Europe”

**Fig. 1** Current seismic hazard zonation map for Greece (EAK, 2003)



(SERA, <http://www.sera-eu.org>). This regional hazard model, which is fully probabilistic, is essentially an update of the previous ESHM13 (Woessner et al., 2015), proposed in the framework of SHARE project (Giardini et al. 2013), and was built upon recently compiled and fully cross-border harmonized datasets, information and models. The source data, input models and output of ESHM20 are online available at the portal of the European Facilities for Earthquake Hazard and Risk ([www.hazard.EFEHR.org](http://www.hazard.EFEHR.org), Haslinger et al. 2022), which will maintain and further develop the model in collaboration with the GEM Foundation and the European Plate Observing System (EPOS).

Apart from the strictly scientific objectives of ESHM20, including the development of the actual updated and harmonized model and the support of the European Seismic Risk Model (ESRM20, Crowley et al. 2021), one of the main objectives was to interact with CEN/TC250/SC8, i.e., the subcommittee of national experts that is responsible for the development of Eurocode 8 within the European Committee for Standardization (CEN), as well as with key experts at national level, to ensure the correct information and timely implementation of the ESHM20, and extend the output to serve additional engineering requirements as part of the update and revision of Eurocode 8. Within this context, ESHM20 produced two informative ground shaking maps for rock conditions depicting spatial variability of the two newly proposed parameters  $S_{\alpha,475}$  and  $S_{\beta,475}$ , which will be included in an Annex of the revised Eurocode 8—Part1 (prEN 1998–1-1, 2022), as an “informative and acceptable representation of the seismic hazard in Europe for the return period of 475 years”. However, the actual representation of the seismic hazard in terms of the  $S_{\alpha,475}$  and  $S_{\beta,475}$  parameters for each country will still be provided by the relevant Authorities or the National Annex of each country, either in the form of grid or of seismic zones, along with the other Nationally Determined Parameters (NDPs). Within this context, the present work aims to propose a new seismic hazard zonation map for Greece, for rock conditions, based on the results of ESHM20, for potential adoption by the Greek National Annex of the new version of Eurocode 8. The map is accompanied by all the necessary parameters for the definition of the elastic response spectrum based on the revised Eurocode 8, including a novel site categorization scheme and the respective site amplification factors for the consideration of local site conditions, building on previous efforts of the authors (Pitilakis et al., 2006, 2013, 2019, 2020). It therefore constitutes a complete proposal for the definition of the seismic action in the Greek National Annex, fully in line with the requirements of the revised Part 1 of Eurocode 8 (prEN 1998–1-1, 2022). The proposal is supported by a preliminary investigation of the impact of its potential adoption on the seismic design and risk of the building stock in Greece, to help gain a better insight on how important the imposed differences might be for the end-users and the administration.

## 2 Main ESHM20 features

### 2.1 Main input datasets

The development of ESHM20 (Danciu et al. 2021; 2022; 2024) was based on the compilation and harmonization of different datasets, i.e., earthquake catalogues, active faults, and ground shaking recordings. The main datasets with focus on Greece are summarized in the following, while more details can be found in Danciu et al. (2021):

- Unified earthquake catalogue, consisting of the so-called “historical” catalogue (EPICA, Rovida and Antonucci 2021), covering the years between 1000 CE and 1899, and the “instrumental” catalogue (1900–2014), built upon the EMEC catalogue from Grünthal and Wahlström (2012). The unified earthquake catalogue includes more than 60,000 events. The spatial distribution of the epicentres of the events in the unified earthquake catalogue which are located in Greece and in the surrounding regions is shown in Fig. 2a.
- European Fault-Source Model (EFSM20), developed as an update of the European Database of Seismogenic Faults (EDFS13, Basili et al. 2013). EFSM20 considers two main categories of seismogenic faults, i.e., crustal faults and subduction zones. For Greece, the faults in EFSM20 (Fig. 2b) are mainly the ones compiled by Basili et al. (2013) for the SHARE project, enriched by new datasets for the Gulf of Corinth based on GreDaSS (Caputo and Pavlides 2013) and the Aegean region based on Caputo and Pavlides (2013) and Ganas (2021). Regarding the subduction zones, the geometry of the Hellenic Arc (Fig. 2c) and the Cyprus Arc were revisited (Basili et al. 2020), while the geometry of the Calabrian and Gibraltar Arc were reconstructed.

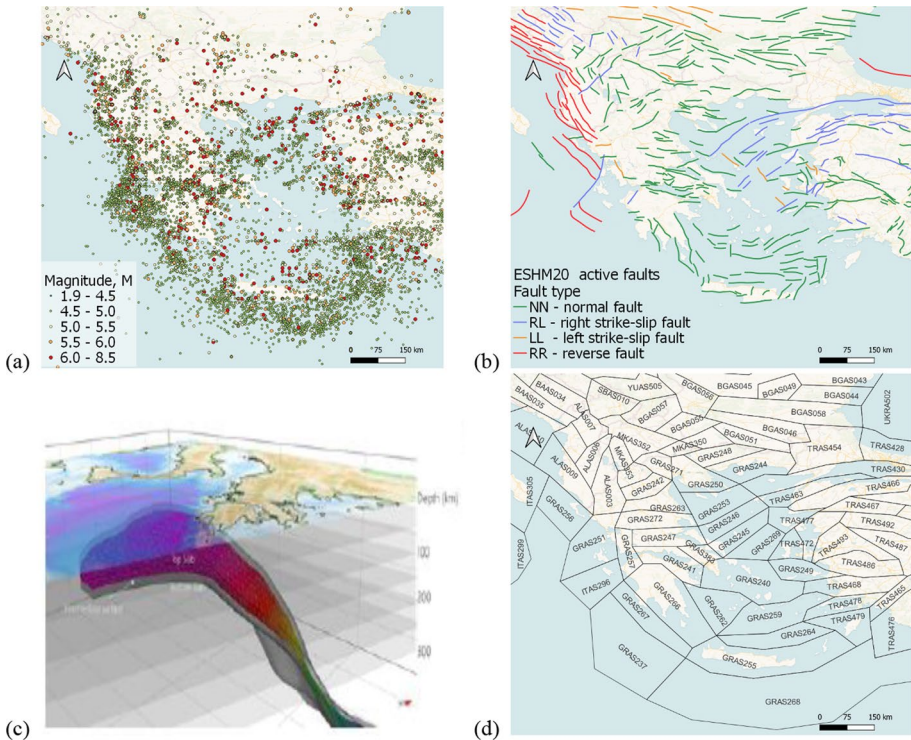


**Fig. 2** EFSM20 datasets for the seismicity of Greece and the surrounding areas **a** unified earthquake catalogue, **b** active faults, **c** subduction zone (Hellenic Arc) (Basili et al. 2020, taken from Danciu et al. 2021), **d** area sources

## 2.2 Seismogenic source model

The inherent uncertainties in characterizing the earthquake rupture forecast are handled by a complex seismogenic source logic tree, consisting of two main branches: an area source-based model, assumed to be the pan-European consensus model with full cross-border harmonization (e.g. Figure 2d for Greece and the surrounding areas), and a hybrid seismicity model that combines the updated active faults datasets with the background seismicity in regions where active faults are identified. The seismogenic source logic tree is supplemented with the subduction zones (i.e., Gibraltar, Calabrian, Hellenic and Cyprus Arcs) and the deep seismicity sources in Vrancea, Romania and the southern Iberia Peninsula. The higher branching levels refer to the magnitude-frequency distribution, the Gutenberg-Richter parameters, slip rates and maximum magnitudes. Further details may be found in Danciu et al. (2021; 2024).

## 2.3 Ground motion model

The ESHM20 ground motion model (GMM) (Kotha et al. 2020; 2022; Weatherill et al 2020, 2023; Weatherill and Cotton 2020) was built around the concept of a scaled backbone ground motion model logic tree (Douglas 2018) in which a single ground motion model is calibrated, and adjustment factors are then applied to this model to quantify the uncertainty in the expected ground motion. The backbone GMM for shallow crustal seismicity (Kotha et al. 2020) was constructed based on the information in the Engineering Strong Motion (ESM) flatfile (Lanzano et al. 2018). Similarly, for the subduction regions, the so-called “BC-Hydro” ground motion model by Abrahamson et al. (2016) was used as backbone GMM.

## 2.4 Seismic hazard results

For different return periods, the seismic hazard results of ESHM20 are provided for a total number of 97,920 geo-located grid points, equally spaced at 0.1 to 0.1 degrees across Euro-Mediterranean region. For each grid point, the following output is provided: (a) hazard curves depicting the mean, median (50th), and four percentiles (5, 16, 84, and 95th) for specified intensity measures (PGA and spectral acceleration values  $S_a$  at periods in the range of 0.05 to 5 s); (b) Uniform Hazard Spectra (UHS) depicting the mean, median (50th) and four percentiles (5, 16, 84, and 95th) for five mean return periods RP (50, 475, 975, 2500 and 5000 years). In addition, hazard maps are provided for all intensity measure types, all statistical metrics and all return periods. For example, the spatial distribution of median PGA and  $S_a(0.3\text{ s})$  for Greece for a return period of 475 years is shown in Fig. 3. Additionally, indicative results in terms of hazard curves and UHS for five of the 61 cities shown in Fig. 4 are shown in Fig. 5. These 61 cities, which may be considered as the most important in Greece in terms of population and socio-economic importance, will be used also in the following section as test sites for the validation of the proposed seismic hazard map.



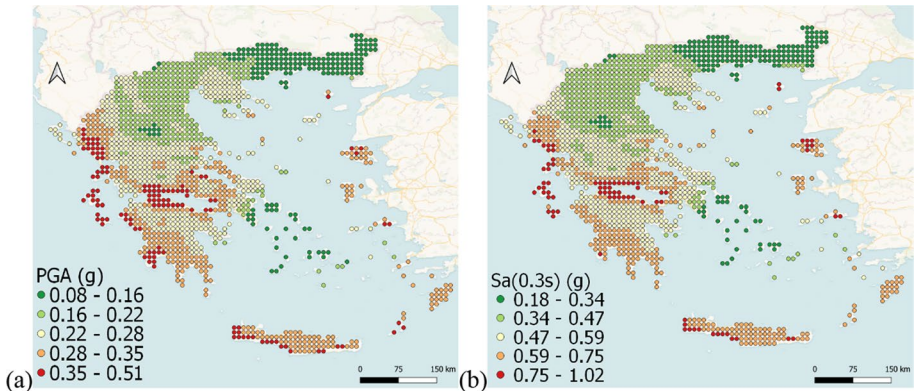


**Fig. 3** Spatial distribution of **a** the median PGA and **b** the median  $S_a(0.3\text{ s})$  value for a return period of 475 years, obtained from ESHM20 for Greece

**Fig. 4** Selected cities in Greece



### 3 Spatial analysis of the ground shaking estimates for seismic zonation of Greece

#### 3.1 Methodology

In the revised Part 1 of EC8 (prEN 1998–1-1, 2022), the elastic response spectrum for a specific return period (RP), instead of being anchored with only one parameter, namely the Peak Ground Acceleration, PGA, is anchored with two parameters,  $S_\alpha$ , which is the spectrum value at the acceleration spectral plateau spanning over a certain spectral period range, and  $S_\beta$ , which is the spectrum value at  $T_\beta = 1\text{ s}$ , more representative for flexible structures (Fig. 6).  $S_\alpha$  is linked with PGA through parameter  $F_A$ , defined as the ratio of  $S_\alpha$  to PGA and set equal to 2.5 in the absence of specific seismic hazard studies. Based on the results of ESHM20, the  $F_A$  parameter for Greece ranges between 2.14 and

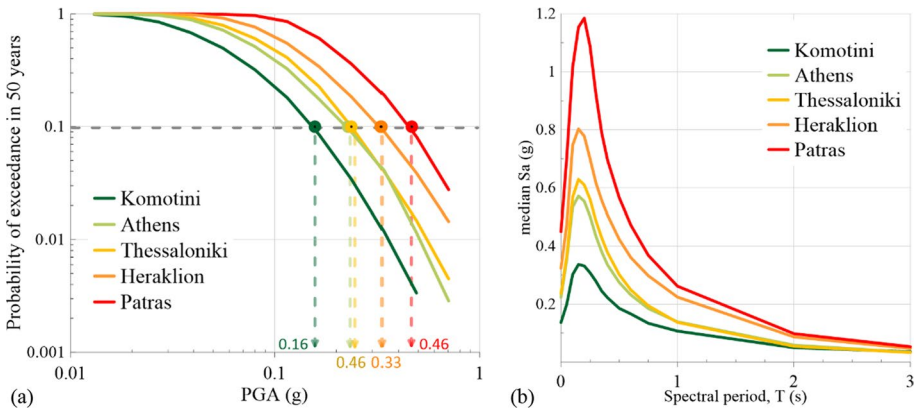
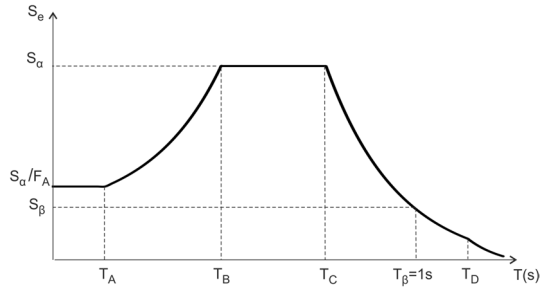


**Fig. 5** **a** Hazard curves and **b** Uniform Hazard Spectra for the cities of Komotini, Athens, Thessaloniki, Heraklion and Patras. For the exact location of the cities, the reader is referred to Fig. 4

2.54, with a mean value of 2.38 and a standard deviation of 0.06, thus the proposed value of 2.5 may be considered as reasonably justified. The  $S_{\beta}$  parameter strongly influences the shape of the normalized response spectrum, as it affects the corner period  $T_C = \frac{S_{\beta} T_{\beta}}{S_a}$ , which specifies the end of the constant spectral acceleration branch of the spectrum (Fig. 6). The definition of the elastic response spectrum in the revised EC8 with two parameters ( $S_{\alpha}$  and  $S_{\beta}$ ) is in line with the recent developments in the definition of seismic actions, including NEHRP seismic code provisions in the U.S.A. (FEMA, 2015). The  $S_a$  and  $S_{\beta}$  parameters for a return period (i.e., RP) are obtained from the respective values at rock conditions (site category A,  $V_s > 800$  m/s),  $S_{a,RP}$  and  $S_{\beta,RP}$ , multiplied by the short-period ( $F_{\alpha}$ ) and intermediate-period ( $F_{\beta}$ ) site-amplification factors, respectively, to account for the effect of local site conditions. Four corner periods are further needed to fully define the shape of the elastic response spectrum (Fig. 6);  $T_A$  is the short-period cut-off associated with the zero-period spectral acceleration which marks the beginning of the ascending branch and is set equal to 0.05 s,  $T_B$  and  $T_C$  are the lower and upper corner periods of the constant spectral acceleration range, while  $T_D$  is the corner period at the beginning of the constant displacement response range of the spectrum.

Thanks to the interaction of ESHM20 with CEN/TC250/SC8, the committee in charge of the ongoing revision of Eurocode 8, ESHM20 delivered values of  $S_{\alpha,475}$  and  $S_{\beta,475}$  for the return period of 475 years, used for the design of ordinary buildings, for the whole Europe at a dense grid of points, equally spaced at 0.1 to 0.1 degrees. For each point of the ESHM20 grid,  $S_{\alpha,475}$  and  $S_{\beta,475}$  were computed from the respective UHS. For the computation of  $S_{\alpha,475}$ , for each grid point of ESHM20, the spectral period  $T_{peak}$  that corresponds to the peak of the median UHS is first identified and then,  $S_{\alpha,475}$  is calculated as the average spectral value over the range of periods between  $0.5T_{peak}$  and  $1.5T_{peak}$  (Labbé and Paolucci 2022).  $S_{\beta,475}$  is directly the UHS value for a spectral period of 1.0 s. The two ground shaking maps will be included in an Annex of prEN 1998–1-1 (2022), as an “informative and acceptable representation of the seismic hazard in Europe for the return period of 475 years”. The spatial distribution of median  $S_{\alpha,475}$  and  $S_{\beta,475}$  for Greece is shown in Fig. 7. These maps include only the terrestrial grid points of the Greek territory, while maps with additional offshore grid points are also available.

**Fig. 6** Shape of the elastic response spectrum of the revised Eurocode 8



Although  $S_{\alpha,475}$  and  $S_{\beta,475}$  are available at a dense grid, it has been shown that due to specific seismotectonic features the differences in close distances might be very important, a fact which could produce important societal and economic problems. Hence, we decided that for common engineering applications, as is a seismic code in force, it would be more appropriate to provide to the engineering community zones of equal seismic hazard, as is the current practice in Greece and other countries worldwide (e.g. Portugal, Romania and Spain). In addition, considering that the revised Eurocode 8 has two seismic hazard parameters ( $S_{\alpha,475}$  and  $S_{\beta,475}$ ) instead of one, and consequently one might consider reasonable having two zonation maps distinct for the two parameters, we based the proposed zonation on one of them, i.e.  $S_{\alpha,475}$ , as this parameter is more crucial for the most common building typologies in Greece, and, as we will describe in more detail in the following, we used the same zones providing adequate values for  $S_{\beta,475}$ .

Following the rationale of the current seismic hazard map in force, we first made an attempt to divide the Greek territory into three seismic zones using the  $S_{\alpha,475}$  parameter shown in Fig. 7a. To this end, we applied the Natural Breaks (Jenks 1967) algorithm, available in the open-source GIS software QGIS, which tries to find natural groupings of data to create classes so that the variance between individual classes is maximized, while the variance within each class is minimized. The resulting zonation is shown in Fig. 8a.

For each of the zones in Fig. 8a, we calculated the average  $S_{\alpha,475}$  value over the grid points located in each zone. The resulting average  $S_{\alpha,475}$  values are 0.38 g for Zone 1, 0.6 g for Zone 2 and 0.83 g for Zone 3. Given that the main seismic hazard parameter used in

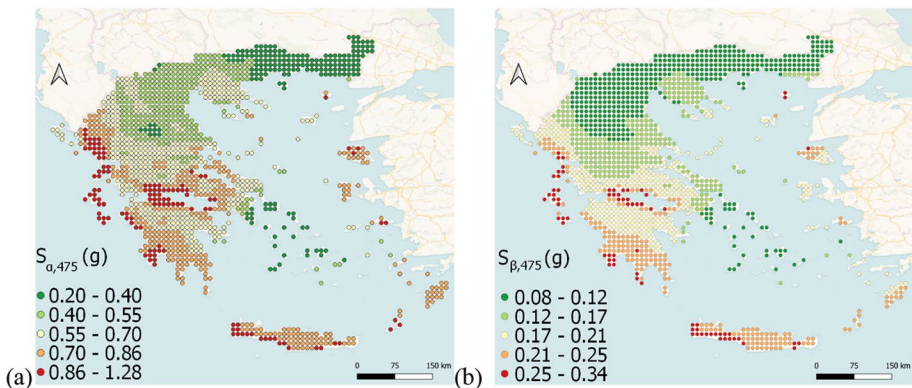


**Fig. 7** Spatial distribution of **a** median  $S_{\alpha,475}$ , and **b** median  $S_{\beta,475}$  derived from ESHM20 for Greece



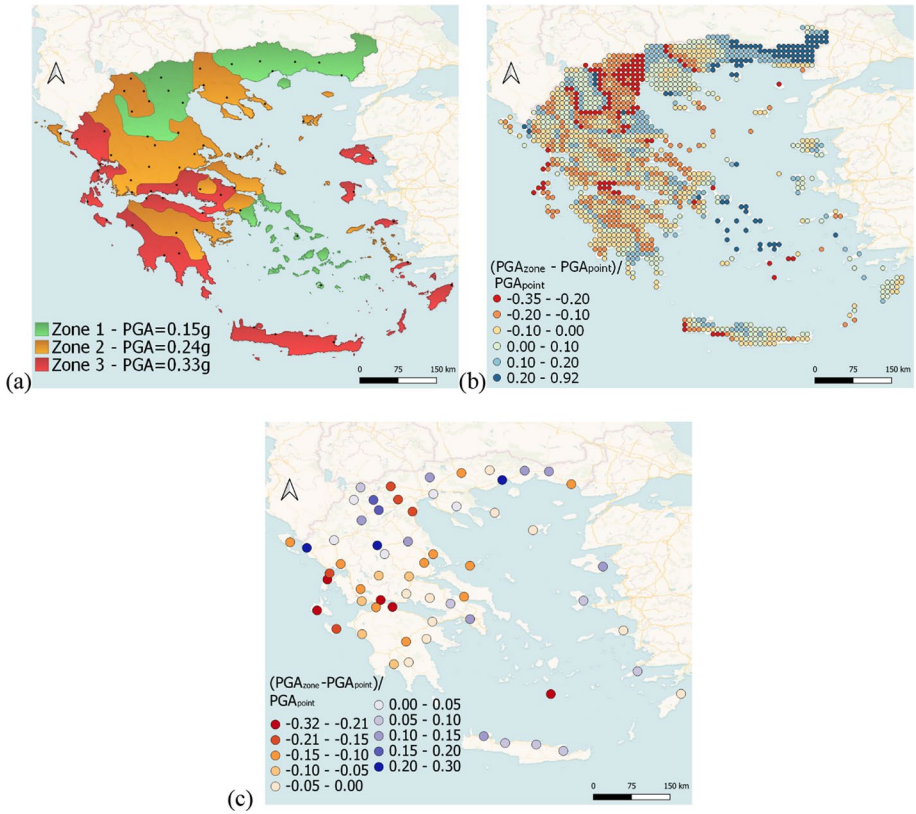


**Fig. 8** **a** Three-zone seismic hazard map for Greece based on ESHM20. The legend indicates the average PGA value for each zone,  $PGA_{zone}$ , calculated as the average of the  $S_{\alpha,475}/2.5$  ratios of the grid points within each zone. **b**  $(PGA_{zone} - PGA_{point})/PGA_{point}$  ratios at the terrestrial grid points of ESHM20 in Greece. **c**  $(PGA_{zone} - PGA_{point})/PGA_{point}$  ratios for the 61 biggest cities in Greece.  $PGA_{point}$  is calculated as  $S_{\alpha,475}/2.5$

seismic codes for decades has been PGA, we also calculated for each zone an average PGA, as the average of the  $S_{\alpha,475}/2.5$  values of the grid points within each zone, herein referred to as  $PGA_{zone}$ , so that the hazard levels of the zones can be more easily perceived by the engineering community. The resulting average  $\pm$  one standard deviation  $PGA_{zone}$  values are  $0.15 \pm 0.03$  g for Zone 1,  $0.24 \pm 0.03$  g for Zone 2 and  $0.33 \pm 0.04$  g for Zone 3, not very far from the PGA values of the hazard map in force (with proposed values of 0.16 g for Zone 1, 0.24 g for Zone 2 and 0.36 g for Zone 3). However, the geographic boundaries of the zones are quite different. For example, Zone 3 in the current seismic map is limited to the Ionian islands (Fig. 1), while in Fig. 8a it extends to the western Peloponnese, the Gulf of Corinth, Crete, and the islands of eastern Aegean. We should note here that at this stage we applied the Natural Jenks algorithm also on another dataset which includes additionally the offshore grid points of the Greek territory and a comprehensive number of grid points located in the bordering countries, at the northern and eastern cross border region of Greece, i.e. Turkey, Bulgaria, North Macedonia and Albania. The resulting zonation was very similar to the one shown in Fig. 8a, so in the following we used only the terrestrial grid points.

Keeping in mind that we want to propose a zonation that is representative of ESHM20, we proceeded with checking how much the computed  $PGA_{zone}$  values of each zone (calculated as the average of the  $S_{\alpha,475}/2.5$  ratios of the grid points within each zone) deviate from the actual  $S_{\alpha,475}/2.5$  ratios of the ESHM20 grid points ( $PGA_{point}$ ). We, therefore, calculated as a measure for this deviation the  $(PGA_{zone} - PGA_{point})/PGA_{point}$  ratios for all the terrestrial grid points of ESHM20 (Fig. 8b). In addition, we interpolated the  $PGA_{point}$  values ( $S_{\alpha,475}/2.5$ ) of ESHM20 to obtain the  $PGA_{point}$  values for the locations corresponding to the 61 major Greek cities shown in Fig. 4, and then calculated the  $(PGA_{zone} - PGA_{point})/PGA_{point}$  ratios for these cities as well (Fig. 8c). The exact values for this ratio for the 61 cities are provided in Table 8 of the Appendix. Negative or positive values of the ratio mean that the zonation of Fig. 8a underestimates or overestimates PGA with respect to ESHM20 grid output, respectively. For 21 of these cities the ratio is less than  $-10\%$ , and in some cases as Aigio, Argostoli and Santorini it is even less than  $-25\%$ , which means that the proposed zonation underestimates the seismic hazard in these regions to a significant extent.

For this reason, it was deemed necessary to move to a zonation map with additional zones. At this stage a threshold was set for the acceptable  $(PGA_{zone} - PGA_{point})/PGA_{point}$  ratio based on the population and the general importance of each city, assuming stricter criteria for the cities with the highest population (Table 1). Based on these criteria, the zonation was modified with the addition of one more zone, leading to the four-zone map of Fig. 9a. The borders of the zones in this map were further smoothed so that they do not cross large urban areas with more than 2,000 buildings, while specific areas belonging in the same administrative units were harmonized to simplify the application of the seismic regulations in these regions. The average  $\pm$  one standard deviation  $PGA_{zone}$  values over the points located within Zones 1–4 in the four-zone map of Fig. 9a are  $0.12 \pm 0.02$  g for Zone 1,  $0.20 \pm 0.03$  g for Zone 2,  $0.28 \pm 0.04$  g for Zone 3 and  $0.37 \pm 0.04$  g for Zone 4. The process of comparing the  $(PGA_{zone} - PGA_{point})/PGA_{point}$  ratios with the acceptable thresholds of Table 1 needed to be repeated for the four-zone map, as  $PGA_{zone}$  values were altered. According to Fig. 9c and Table 9 in the Appendix, in the four-zone map there are fewer but still several locations (cities) where the proposed zonation underestimates (negative ratios) or overestimates (positive ratios) the seismic hazard compared to the closest ESHM0 grid point.

A final iteration was repeated using five zones instead of four (Fig. 10a), for which the average  $\pm$  one standard deviation  $PGA_{zone}$  values are  $0.13 \pm 0.02$  g for Zone 1,  $0.19 \pm 0.02$  g for Zone 2,  $0.23 \pm 0.02$  g for Zone 3,  $0.29 \pm 0.04$  g for Zone 4 and  $0.37 \pm 0.04$  g for Zone 5. The threshold criteria for the  $(PGA_{zone} - PGA_{point})/PGA_{point}$  ratios of Table 1 are met for all the 61 major cities (Fig. 10c and Table 10 of the Appendix), so the iteration process was considered satisfied and hence stopped. The optimum zonation is therefore the five-zone map of Fig. 10a and is proposed to be applied for both the  $S_{\alpha,475}$  and  $S_{\beta,475}$  seismic hazard

**Table 1** Threshold values for the acceptable  $(PGA_{zone} - PGA_{point})/PGA_{point}$  ratio for different population classes

Population class	Threshold values for $(PGA_{zone} - PGA_{point})/PGA_{point}$
$\leq 100,000$	$\pm 20$
100,000–500,000	$\pm 15$
$\geq 500,000$ –1,000,000	$\pm 10$

$PGA_{zone}$  is calculated as the average of the  $S_{\alpha,475}/2.5$  ratios of the grid points within each zone PGA, while  $PGA_{point}$  is calculated as  $S_{\alpha,475}/2.5$

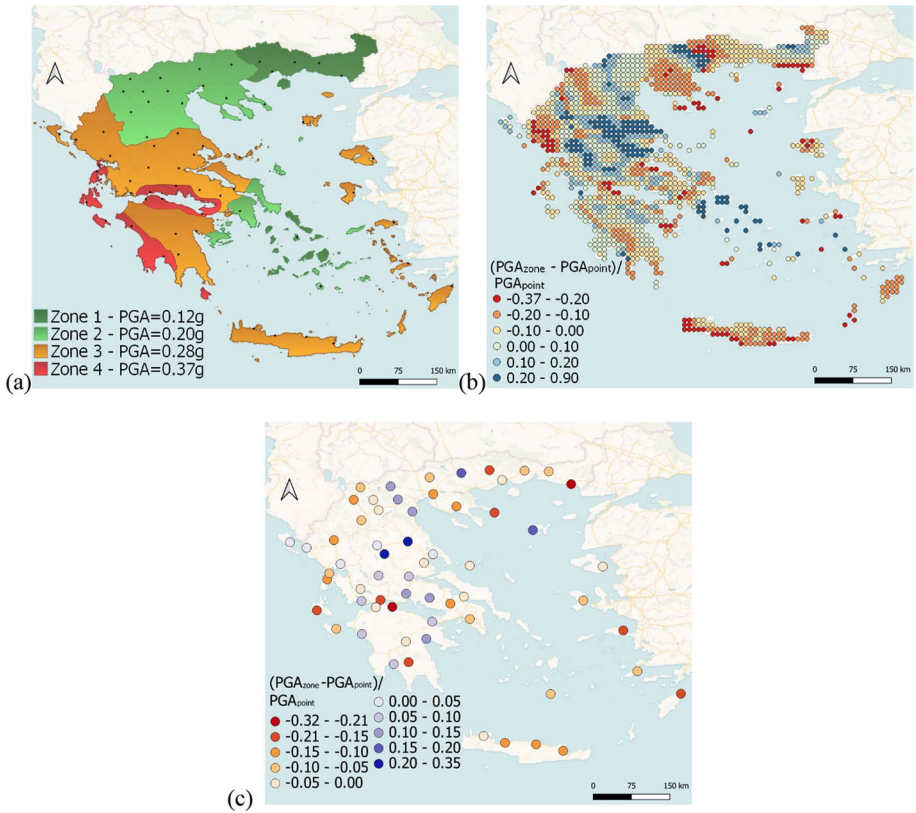


**Fig. 9** **a** Four-zone seismic hazard map for Greece based on ESHM20. The legend indicates the average PGA value for each zone,  $PGA_{zone}$ , calculated as the average of the  $S_{\alpha,475/2.5}$  ratios of the grid points within each zone. **b**  $(PGA_{zone} - PGA_{point})/PGA_{point}$  ratios at the terrestrial grid points of ESHM20 in Greece. **c**  $(PGA_{zone} - PGA_{point})/PGA_{point}$  ratios for the 61 biggest cities in Greece.  $PGA_{point}$  is calculated as  $S_{\alpha,475/2.5}$

parameters, to ensure an easier application of the map by the engineering community. We should note here that the proposed  $PGA_{zone}$  for Zone 1 (0.13 g) is less than the minimum PGA in the current seismic hazard map of Greece (0.16 g for Zone 1, Fig. 1). In the case of a potential official adoption of this proposal by the Greek National Annex of the new Eurocode 8, the authorities may need to consider increasing this value to at least 0.16 g, as a reduction of design values would result in liability issues for the decision makers and the designers.

From Figs. 8, 9 and 10 it is clear that the transition from three to five zones results in a significant improvement of the proposed seismic hazard map in terms of agreement with the ESHM20 output, as the adopted thresholds for the  $(PGA_{zone} - PGA_{point})/PGA_{point}$  ratios are satisfied for all major cities at the five-zone map. Few grid points with ratios less than -20% in Fig. 10b (e.g. in southwest Crete) refer to mostly rural regions with small population. In the following, we provide an indicative result to demonstrate how this iterative process improved the proposed seismic hazard map in terms of the adopted criteria for the  $(PGA_{zone} - PGA_{point})/PGA_{point}$  ratios. For the city of Aigion, known for its high seismicity and located at the coastline of the Corinthian Gulf, for the three-zone map (Fig. 8a) the

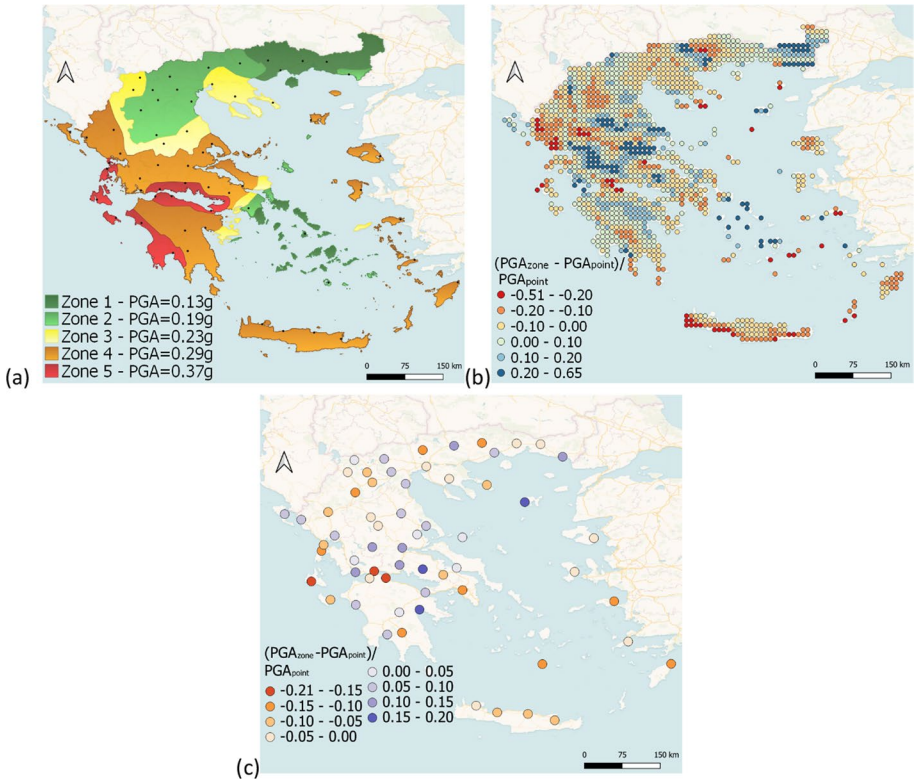


**Fig. 10** **a** Five-zone seismic hazard map for Greece based on ESHM20. The legend indicates the average PGA value for each zone,  $PGA_{zone}$ , calculated as the average of the  $S_{\alpha,475/2.5}$  ratios of the grid points within each zone. **b**  $(PGA_{zone} - PGA_{point})/PGA_{point}$  ratios at the terrestrial grid points of ESHM20 in Greece. **c**  $(PGA_{zone} - PGA_{point})/PGA_{point}$  ratios for the 61 biggest cities in Greece.  $PGA_{point}$  is calculated as  $S_{\alpha,475/2.5}$

$(PGA_{zone} - PGA_{point})/PGA_{point}$  ratio is about  $-29\%$  (Table 8 in the Appendix), higher than the  $\pm 20\%$  threshold based on the population of the city (see Table 1), meaning that this zonation underestimates seismic hazard at this location compared to the closest ESHM20 grid point and the adopted thresholds. Moving to the four-zone map (Fig. 9a), this ratio is reduced to  $-21\%$  (Table 9 in the Appendix), still exceeding the adopted threshold, while for the five-zone map (Fig. 10a) this ratio is further decreased to  $-19.5\%$  (Table 10 in the Appendix) and the criterion is satisfied. Further increase of the seismic zones to reduce the deviation is considered ineffective for practical reasons and because it might create important collateral effects in several regions.

### 3.2 Proposed ground shaking zonation for Greece

The proposed ground shaking zonation map for Greece is shown at a larger scale in Fig. 11. Zone 1, the one with the lowest seismic hazard level, contains Thrace (except for the area around the city of Alexandroupoli), the eastern part of Attica, and the islands of Cyclades. Zone 2 contains the greatest part of central and western Macedonia, northern Thessaly as well as the central part of Attica. Zone 3 acts as a transition zone between the low-hazard



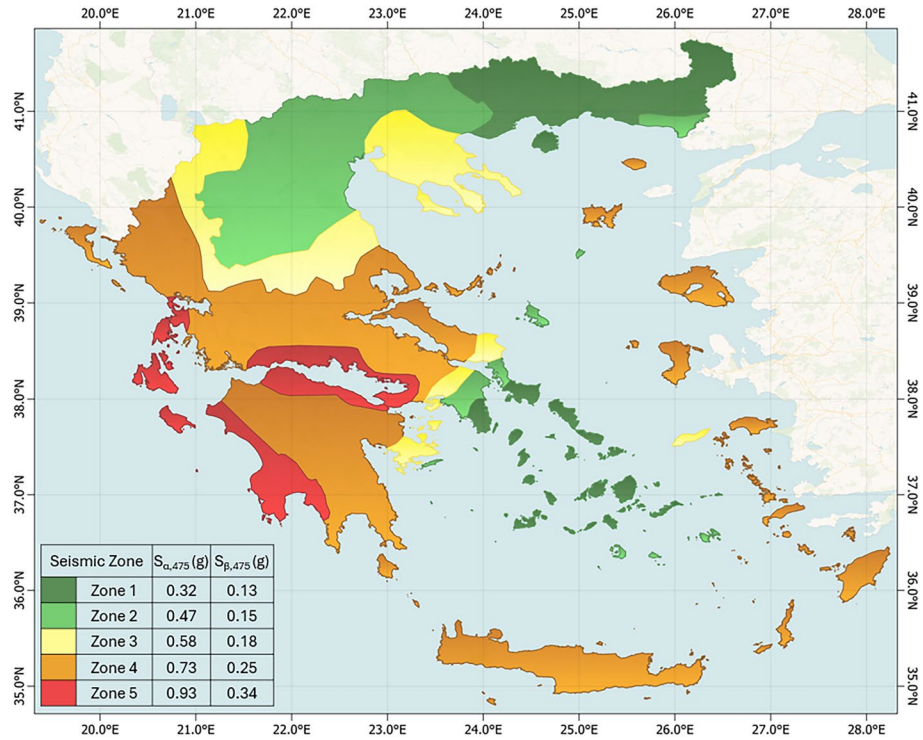


**Fig. 11** Proposed seismic hazard zonation based on the ESHM20 ground shaking estimates for a mean return period of 475 years. The proposed  $S_{\alpha,475}$  and  $S_{\beta,475}$  for each zone are given in the legend of the figure

Zone 2 and the higher-hazard Zone 4 in Thessaly and Attica, while it also covers the city of Thessaloniki and Chalkidiki, regions which historically exhibited very strong earthquakes. Zone 4 includes western Greece except for the Ionian islands, the greatest part of central Greece and Peloponnese, Crete and the island of eastern Aegean, while Zone 5 refers to the Ionian islands, the Corinth Gulf and western Peloponnese. This map is actually consistent with the well-known and documented seismic history of these areas, while it considers the importance of the population density and the general importance of the cities and the regions.

For a potential adoption of the map by the National Annex of the revised EC8, it should be accompanied by appropriate  $S_{\alpha,475}$  and  $S_{\beta,475}$  values for each one of the five zones. Regarding  $S_{\alpha,475}$ , given that the map was developed based on the spatial distribution of the median  $S_{\alpha,475}$  values of the grid points located in Greece, an average of the median  $S_{\alpha,475}$  values over the grid points located within each zone was assigned to each zone. These values are provided for each zone in the legend of Fig. 11, as well as in Table 2. Accepting that the same map applies for both parameters and applying for  $S_{\beta,475}$  the same rationale as for  $S_{\alpha,475}$ , i.e. averaging the median  $S_{\beta,475}$  values over the grid points located within each zone, the resulting elastic response spectra for rock (soil type A) have a very narrow width of the constant-acceleration branch, a result of the low values of  $T_C = \frac{S_{\beta} T_{\beta}}{S_a}$ . For this reason, we investigated the use of higher percentiles than the 50th (median). Besides, the use of higher percentiles allows for better accounting of the epistemic uncertainties of the ground



**Table 2** Proposed values per zone for the elastic spectrum parameters of the new Eurocode 8 for rock-type conditions and a return period of 475 years

Seismic zone	$S_{\alpha,475}$ (g)	$S_{\beta,475}$ (g)	PGA (g)	$T_A$ (s)	$T_B$ (s)	$T_C$ (s)	$T_D$ (s)
Zone 1	0.32	0.13	0.13	0.02	0.10	0.41	2.28
Zone 2	0.47	0.15	0.19	0.02	0.08	0.32	2.47
Zone 3	0.58	0.18	0.23	0.02	0.08	0.31	2.77
Zone 4	0.73	0.25	0.29	0.02	0.09	0.35	3.45
Zone 5	0.93	0.34	0.37	0.02	0.09	0.36	4.34

motion models and the seismogenic sources at lower frequencies, which in the case of Greece are very high due to the very complex seismo-tectonic context of the region. An example of adopting different percentiles for  $S_{\beta,475}$  is shown in Fig. 12, which compares for the proposed Zone 4 of Fig. 11 the elastic response spectra for soil type A (rock conditions) based on the revision of Eurocode 8 (prEN 1998–1-1, 2022) using the average  $S_{\beta,475}$  value over the grid points located in this zone obtained (a) from the median  $S_{\beta,475}$  map (orange dashed line) and (b) from the 84th percentile  $S_{\beta,475}$  map (orange solid line). The elastic response spectra for soil type A for seismic Zone 2 according to the current EC8 (EN 1998–1, 2004) as well as EAK 2003 are also included in Fig. 12 for the sake of comparison. We observe that the use of the median  $S_{\beta,475}$  results in a spectrum with a significantly narrower branch of constant acceleration (plateau) compared to the seismic codes in force (i.e., EAK 2003 and current EC8), which in its turn would result in a significant decrease of seismic force for buildings with spectral periods higher than 0.4 s, including many typical 3–8-storey buildings in Greece. For this reason, we decided to adopt the use of the 84th percentile  $S_{\beta,475}$ , which results in spectrum shapes which are more consistent with the current practice and know-how, respecting at the same time the seismogenic and ground motion features of the region.

The distributions of (a) the median  $S_{\alpha,475}$  values, and (b) the 84th quantile of  $S_{\beta,475}$  values for the five zones of the proposed new seismic hazard map of Fig. 11 are shown in Fig. 13, where we depict the ranges as well as the average  $\pm$  one standard deviation values for the two parameters. Standard deviations range between 0.06 and 0.10 for median  $S_{\alpha,475}$  and between 0.02 and 0.09 for 84th quantile of  $S_{\beta,475}$ , with the higher values observed for the two zones with the highest seismicity, i.e. Zones 4 and 5. In general, the patterns between the  $S_{\alpha,475}$  and  $S_{\beta,475}$  distributions are similar for all five zones, which further supports the proposal for common zonation for the two seismic hazard parameters.

The proposed  $S_{\alpha,475}$  and  $S_{\beta,475}$  values for the five zones of the seismic map are included in the legend of Fig. 11, as well as in Table 2. Table 2 further includes for each zone the PGA value for rock conditions (equal to  $S_{\alpha,475}/F_A$ ), as well as the four corner periods  $T_A$ ,  $T_B$ ,  $T_C$ ,  $T_D$  as obtained from the respective equations of the revised EC8, again for rock conditions (soil type A).  $T_A$  is set equal to 0.05 s,  $T_D$  is equal to 2.0 s if  $S_{\beta,475} \leq 1$  m/s<sup>2</sup>, otherwise it is defined as  $1 + S_{\beta,475}$  (in m/s<sup>2</sup>),  $T_C$  is equal to the  $S_{\beta}/S_{\alpha}$  ratio and  $T_B$  is dependent on  $T_C$  and a parameter  $\chi$  equal to 4 (prEN 1998–1-1:2022). It is noted that the values of the parameters included in Table 2 for each zone are the exact values obtained from the application of the adopted methodology. However, in the case of a potential official adoption of this proposal by the Greek National Annex of the new Eurocode 8, these values could be rounded to ensure an easier application by the practitioners. In addition, for Zone 1, the slightly higher values of PGA (and equivalent  $S_{\alpha,475}$  and  $S_{\beta,475}$ ) of the present zonation map could be retained.

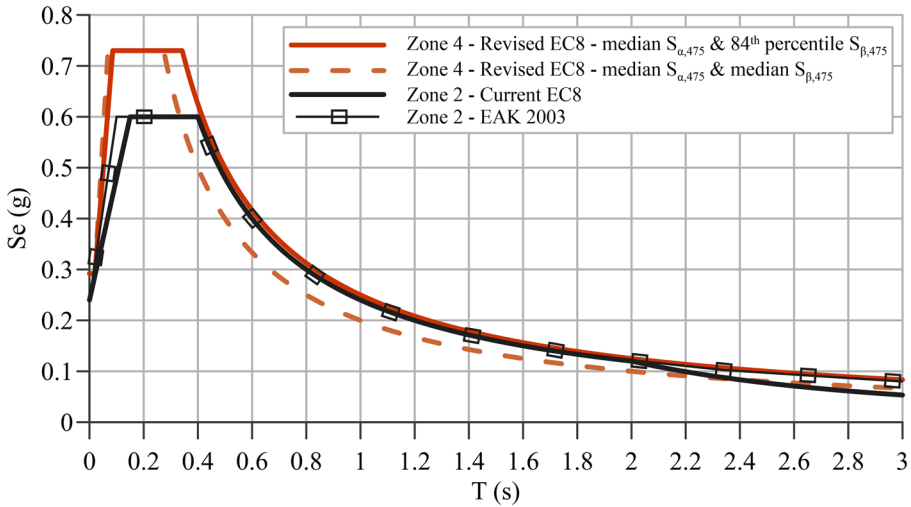


**Fig. 12** Elastic response spectra for soil type A for Zone 4 of the proposed hazard map based on the revision of Eurocode 8 (prEN 1998–1-1, 2022) considering median  $S_{\beta,475}$  (orange dashed line) and the 84th percentile  $S_{\beta,475}$  (orange solid line), and elastic response spectra of the current EC8 (black solid line) and EAK 2003 (black dotted line) for Zone 2 of the current seismic map

### 4 Site categorization

As already mentioned in Sect. 3, the revised EC8 (prEN 1998–1-1, 2022) accounts for the effect of local site conditions through the short-period ( $F_\alpha$ ) and intermediate-period ( $F_\beta$ ) site-amplification factors. Site-amplification factors are dependent on the site category, which is based on two parameters, namely  $H_{800}$  (depth of the conventional bedrock formation, identified by a shear wave velocity at least equal to 800 m/s) and  $V_{s,H}$  (time-averaged shear wave velocity of the top 30 m or down to  $H_{800}$  if  $H_{800} < 30$  m). Based on the site category, prEN 1998–1-1 (2022) provides appropriate analytical expressions for the computation of  $F_\alpha$  and  $F_\beta$ , introducing a dependency not only on the site class but also on the level of seismic ground motion in order to account for the non-linear behavior of the soils. Alternatively, default intensity-dependent values of  $F_\alpha$  and  $F_\beta$  are introduced for the cases

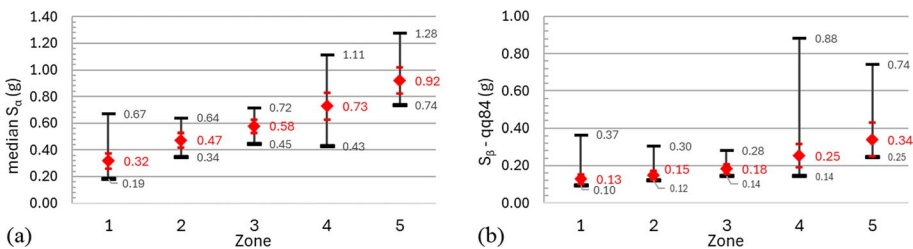


**Fig. 13** Distribution of **a** the median  $S_{\alpha,475}$  values, and **b** the 84th quantile of  $S_{\beta,475}$  values for each zone of the proposed seismic hazard map. Red diamonds depict the average values, red dashes depict the average  $\pm$  one standard deviation values and the black dashes represent the minimum and the maximum values

where a simplified identification of the site category is adopted because of insufficient geotechnical information.

This procedure for the determination of the site class and the respective amplification factors included in the revised EC8 is probably not very straightforward, requiring besides the knowledge of  $H_{800}$  which is quite ambiguous in most cases, the use of different tables and equations located at different parts of the code, depending on the availability or not of the necessary information. This could potentially lead in practice to a simple adoption of the default amplification factors by the engineers which constitutes an oversimplification. Given that each country may adopt different standards for site categorization and estimation of site amplification in its National Annex, and taking advantage of a series of previous work conducted in the framework of site categorization for seismic codes (Pitilakis et al., 2006, 2013, 2019, 2020), we decided to propose for the Greek National Annex the site categorization scheme elaborated by Pitilakis et al. (2020). The proposed scheme, given in Table 3, introduces the approximate depth to seismic bedrock,  $H_B$ , as the main classification parameter in addition to equivalent shear wave velocity  $V_{s,H}$ , which is the time-averaged shear wave velocity of the top 30 m ( $V_{s,30}$ ) if the seismic bedrock is located at a depth greater than 30 m, otherwise it is the time-averaged shear wave velocity down to the depth of bedrock. This means that in all cases where the soil deposits have a thickness greater than 30 m,  $V_{s,H}$  is equal to  $V_{s,30}$ . In addition to  $H_B$  and  $V_{s,H}$ , the fundamental period,  $T_0$ , of the site is used as a supplementary important parameter allowing to better distinguish between specific subclasses. Correlations of soil classes with the time-averaged shear wave velocity of the entire soil deposit down to seismic bedrock,  $V_{s,av}$ , and average values of standard penetration test blow count, N-SPT, and undrained shear strength,  $S_u$  are also provided (Table 3). To obtain  $T_0$  and  $V_{s,H}$  or  $V_{s,av}$ , invasive (in-hole measurements) or non-invasive (e.g. surface-waves analysis) techniques at very small shear strains may be used which are now very low cost. In case of absence of direct measurement parameters, adequate correlations of the  $V_s$  and consequently  $T_0$  with SPT and CPT may be applied (e.g. Athanasopoulos 1994; Mayne and Rix 1995; Anagnostopoulos et al 2003; Idriss and Boulanger 2007.).

For the site amplification factors  $F_\alpha$  and  $F_\beta$  we propose the intensity-dependent amplification factors proposed by Pitilakis et al. (2020), adjusted for the  $S_{\alpha,475}$  levels defined for the five zones of the proposed seismic hazard map. In this way, a single  $F_\alpha$  and a single  $F_\beta$  value are derived for each soil class and for each zone (Table 4). This procedure for the determination of  $F_\alpha$  and  $F_\beta$  is in our opinion more straightforward and easier to be applied in engineering practice compared to what is proposed in the revised EC8. It is again noted that the  $F_\alpha$  and  $F_\beta$  values given in Table 4 are the exact values obtained from the application of the adopted methodology. However, in the case of a potential official adoption of this proposal by the Greek National Annex of the new Eurocode 8, the values of Table 4 can be rounded to ensure an easier application by the practitioners.

The short-period amplification factors  $F_\alpha$  are directly comparable to the soil amplification factors,  $S$ , of the current EC8 (EN 1998–1, 2004), as the spectral plateau in EC8 spectra is amplified by  $S$ . The herein proposed values of  $F_\alpha$  for soil classes B1 and B2 are quite close to the  $S$  value of 1.2 for EC8 soil class B, contrary to the proposed  $F_\alpha$  values for soil classes C1, C2 and C3, which are significantly higher than the  $S$  factors of EC8 soil classes B ( $S$  equal to 1.2) and C ( $S$  equal to 1.5), mainly for the low hazard Zones 1 and 2. The proposed values for  $F_\alpha$  are higher in the cases of soil classes D and E as well, as the respective EC8  $S$  factors are 1.35 and 1.4 respectively. The intermediate-period amplification factors  $F_\beta$  can be compared with the spectral ratios of the normalized EC8 spectrum for each soil type to the normalized EC8 spectrum for soil type A for  $T=1$  s, which are equal to 1.5,

**Table 3** Proposed soil categorization system

Site class	Description	$H_B$ (m)	$V_{s,H}$ (m/s)	$T_0$ (s)	Remarks
A	-Rock -Slightly weathered/segmented rock formations with weathered layer of thickness $z < 5.0$ m	$\geq 800$	$\leq 0.2$	For weathered zone: $z < 5$ m: $V_{s,av} \geq 300$ m/s	
B1	-Weathered/soft rock -Shallow very stiff soil deposits, consisting either of very dense sand/gravel or very stiff to hard clay	$\leq 30$	300–800	$0.2 \pm 0.1$ $V_{s,av}$ : 400–800 m/s N-SPT > 50 $S_u > 150$ kPa	
B2	Intermediate depth stiff soil deposits, consisting either of sand or clay, whose mechanical properties increase with depth	30–60	400–800	$0.4 \pm 0.2$ $V_{s,av}$ : 400–800 m/s N-SPT > 50 $S_u > 150$ kPa	
C1	Deep stiff soil deposits, consisting either of sand/gravel or clay	$> 60$	400–800	$0.6 \pm 0.2$ $V_{s,av}$ : 400–800 m/s N-SPT > 50 $S_u > 150$ kPa	
C2	Intermediate depth soil deposits, consisting of medium dense sand and gravel and/or medium stiffness clay ( $PI > 15$ , fines $> 30\%$ )	20–60	150–400	$0.5 \pm 0.2$ $V_{s,av}$ : 200–500 m/s N-SPT > 20 150 kPa $> S_u > 70$ kPa	
C3	Deep soil deposits, consisting of medium dense sand and gravel and/or medium stiffness clay	$> 60$	250–400	$1.2 \pm 0.5$ $V_{s,av}$ : 300–500 m/s N-SPT > 20 150 kPa $> S_u > 70$ kPa	
D	Deep soil deposits consisting of soft to medium stiffness clays and/or loose sandy to sandy-silt formations with substantial fines percentage (potentially non-liquefiable)	$> 60$	150–250	$2.0 \pm 0.8$ $V_{s,av}$ : 200–400 m/s N-SPT < 20 $S_u < 70$ kPa The dominant soil formations may be interrupted by layers of very soft clays ( $S_u < 25$ kPa, $W > 40\%$ , $PI > 25$ ) or sands and sandy clays of relatively small thickness ( $< 10$ m)	
E	Shallow soil deposits, generally classified as type C2 or D according to its geotechnical properties, which overlie type A formations	$< 20$	150–300	$\leq 0.5$	

**Table 3** (continued)

Site class	Description	$H_B$ (m)	$V_{s,H}$ (m/s)	$T_0$ (s)	Remarks
X	<p>Loose fine sandy-silty soils with high water table, potentially liquefiable</p> <p>Loose granular or soft silty-clayey soils, provided they have been proven to be hazardous in terms of dynamic compaction or loss of strength</p> <p>Soils near obvious tectonic faults</p> <p>Steep slopes covered with loose soil deposits</p> <p>Recent loose landfills</p> <p>Soils with a very high percentage in organic material</p> <p>Peat and/or highly organic clays (<math>H &gt; 3</math> m) and/or very high plasticity clays (<math>H &gt; 8</math> m) and/or very thick, soft/medium stiff clays (<math>H &gt; 30</math> m)</p> <p>Loess</p> <p>Special soils and site conditions requiring site-specific evaluations—not included in types A–E</p>				



**Table 4** Site amplification factors  $F_{\alpha}$  and  $F_{\beta}$

Soil class	Soil amplification factor $F_{\alpha}$					Soil amplification factor $F_{\beta}$					
	Zone 1	Zone 2	Zone 3	Zone 4	Zone 5	Soil class	Zone 1	Zone 2	Zone 3	Zone 4	Zone 5
A	1	1	1	1	1	A	1	1	1	1	1
B1	1.3	1.3	1.27	1.21	1.2	B1	1.1	1.1	1.1	1.1	1.1
B2	1.27	1.21	1.2	1.2	1.2	B2	1.37	1.31	1.3	1.3	1.3
C1	1.67	1.61	1.57	1.51	1.5	C1	1.47	1.41	1.4	1.4	1.4
C2	1.45	1.32	1.27	1.21	1.13	C2	2.15	2.02	1.97	1.91	1.9
C3	1.55	1.42	1.34	1.22	1.2	C3	2.25	2.12	2.07	2.01	2
D	1.65	1.52	1.47	1.41	1.33	D	3.36	3.05	2.91	2.73	2.50
E	1.6	1.6	1.57	1.51	1.5	E	1.1	1.1	1.1	1.1	1.1

1.725, 2.7 and 1.75 for soil types B, C, D and E respectively. The proposed  $F_\beta$  values are higher than the spectral ratios of EC8 for soil classes C2, C3 and D, but lower for all the other soil classes. A comparison of the proposed amplification factors to the ones proposed in the revised EC8 is not always feasible due to inherent differences in the two site classification systems, which do not allow for a straightforward correspondence between the two systems and falls outside the scope of this work. However, both the revised EC8 and our proposal have endorsed the need for an increase of amplification factors for sites classified as type C in the current EC8, as well for an intensity-dependence of the proposed values.

## 5 Elastic response spectra

The ground shaking zonation map with associated elastic response spectrum parameters presented in Sect. 3 and the site categorization scheme with respective site amplification factors given in Sect. 4 constitute a complete proposal for the definition of the seismic action in terms of elastic response spectra, suitable for adoption by the Greek National Annex that will accompany the new version of Eurocode 8, following the requirements set by prEN 1998–1–1 (2022). To better evaluate the impact of a potential adoption of this new proposal for the seismic design actions, referred to in the following as NA 2023, on the seismic design of structures, we compare the elastic response spectra obtained with NA 2023 with the ones of the current EC8 (with the existing National Annex) and EAK 2003.

For comparison reasons the elastic response spectra for the different codes were computed as follows:

- NA2023: We used the definition of the elastic response spectra from prEN 1998–1–1 (2022), combined with the  $S_{\alpha,475}$  and  $S_{\beta,475}$  parameters for rock conditions proposed for the five zones of the seismic hazard map in Fig. 11 (Table 2) and the site amplification factors  $F_\alpha$  and  $F_\beta$  of Table 4. All the other parameters required for the computation of the spectra were obtained from prEN 1998–1–1 (2022).
- EAK 2003: We applied the equations of EAK 2003 with the PGA values of the zonation map in force given in Fig. 1. It is reminded that these PGA values in EAK 2003 refer to the ground surface, i.e., they are not amplified by amplification factors.
- Current EC8: We applied the equations of the current EC8 (EN 1998–1, 2004), with the PGA for rock conditions obtained from the zonation map in force given in Fig. 1, which has been adopted by the Greek National Annex for EC8. Contrary to EAK 2003, these values refer to rock conditions and are therefore amplified with the amplification factors of the current EC8 for Type 1 seismicity.

First, in Fig. 14 we compare the elastic response spectra considering rock conditions per zone of the new map (NA2023). For this, we first need to establish a correspondence between the zones of the seismic map in force (Fig. 1) and the herein proposed map (Fig. 11). This correspondence (Table 5) is not one-to-one, with the exception of the new Zone 1, so the elastic response spectra for Zones 2–5 of NA2023 are compared with more than one spectra of EAK 2003 and EC8 (Fig. 14). The most significant discrepancies are observed for the NA2023 Zones 4 and 5, i.e. the zones with the highest seismic hazard, and mainly concern the values of the maximum spectral acceleration (plateau), which are higher compared to the two current codes. For example, the maximum spectral acceleration  $S_{\alpha,475}$  for a site located in Zone 5 based on NA2023 and Zone 2 based on EAK 2003

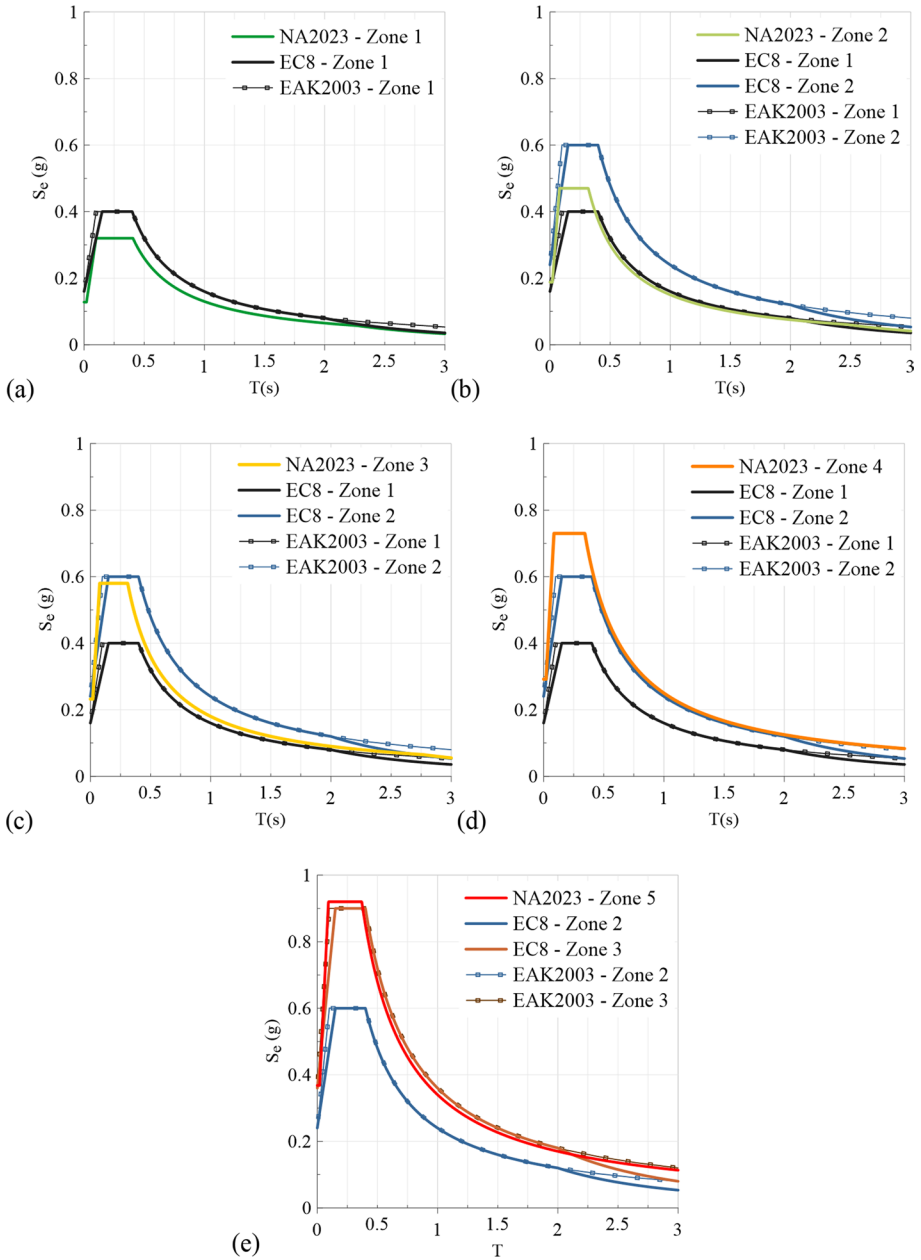


**Fig. 14** Comparison of the elastic response spectra of the proposed zonation (NA2023) for **a** Zone 1, **b** Zone 2, **c** Zone 3, **d** Zone 4 and **e** Zone 5 with the respective spectra of the current version of the Eurocode 8 and EAK 2003 considering rock conditions

(e.g. Patras) is equal to 0.93 g according to NA2023, i.e. 55% higher than it is for EC8 and EAK 2003 (Fig. 14e). The differences are generally lower in higher periods. On the contrary, for the low hazard Zones 1 and 2 the maximum spectral acceleration may decrease

**Table 5** Correspondence between the zones of the proposed seismic hazard map (NA2023) and those of the current seismic hazard map (EAK 2003)

NA2023 zone	EAK2003/ EC8 zone
1	1
2	1, 2
3	1, 2
4	1, 2
5	2, 3

compared to the current codes (Fig. 14a, b). For example, a site in Komotini, located in Zone 1 based on both seismic hazard maps, has a maximum spectral acceleration  $S_{\alpha,475}$  of 0.32 g with NA2023 compared to 0.40 g with EC8/EAK 2003. However, in the case of a potential official adoption of this proposal by the Greek National Annex of the new Eurocode 8, the authorities may need to consider increasing the  $S_{\alpha,475}$  for Zone 1 to a most conservative value corresponding to the current seismic hazard map, as a reduction of design values would result in liability issues for the decision makers and the designers. In general, the discrepancies that have been observed for almost all zones can be attributed to the differences posed by the boundaries of the zones, as well as to the seismic hazard parameters assigned to each zone ( $S_{\alpha,475}$  and  $S_{\beta,475}$  for NA2023, PGA for EC8/EAK 2003).

To additionally investigate the effect of site amplification due to local site conditions on the elastic response spectra, and to overcome the issue of correspondence of the new zones with multiple current zones, we selected five sites located in five different cities, one for each of the new zones, and we assumed local site conditions characterized either as soil type B (for EAK 2003 and EC8) and B1 or B2 for NA2023 (Fig. 15), or soil type C (for EAK 2003 and EC8) and C1, C2 or C3 for NA2023 (Fig. 16). The selected cities are Komotini for Zone 1, the center of Athens for Zone 2, the center of Thessaloniki for Zone 3, Heraklion for Zone 4 and Patras for Zone 5. For the exact location of the cities, the reader is referred to Fig. 4. Again, we observe that in some cases the adoption of the NA2023 proposal may result in significant increase of the seismic demand, as is the case for example for the centre of Thessaloniki (Fig. 15c and 16c), which is due to the increased hazard for rock conditions (PGA equal to 0.23 g based on NA2023 compared to 0.16 g based on EAK 2003), as well as the well proved and documented higher site amplification factors, especially for soil classes C1, C2 and C3 as was noted in Sect. 4. These discrepancies are more pronounced between NA2023 and EAK 2003 due to the complete absence of site amplification in EAK 2003. Similarly to what was observed for the rock conditions, there are some cases where the adoption of the NA2023 elastic spectra results in a decrease of the seismic demand, e.g. for the city of Komotini located in Zone 1 of NA2023. In this case, the NA2023 spectrum values are well below the respective spectra of the current EC8 for the case of soil classes B/B1-B2 (Fig. 15a), mainly due to the lower hazard for rock (0.13 g for NA2023 Zone 1 compared to 0.16 g for EAK 2003 Zone 1) as well as the narrower plateau for NA2023. The differences with EAK 2003 are minimized because of the absence of site amplification in EAK 2003, which counterbalances the difference in the rock hazard. For soil classes C/C1-C2-C3 (Fig. 16a), the NA2023 spectra are above the ones of the current EC8 (and of EAK 2003) due to the higher site amplification factors of NA2023 compared to EC8. These representative results highlight the importance of the effect of local site conditions in the definition of seismic action, which is a fact that cannot be denied. Finally, a general remark is that the majority of the increase in the seismic

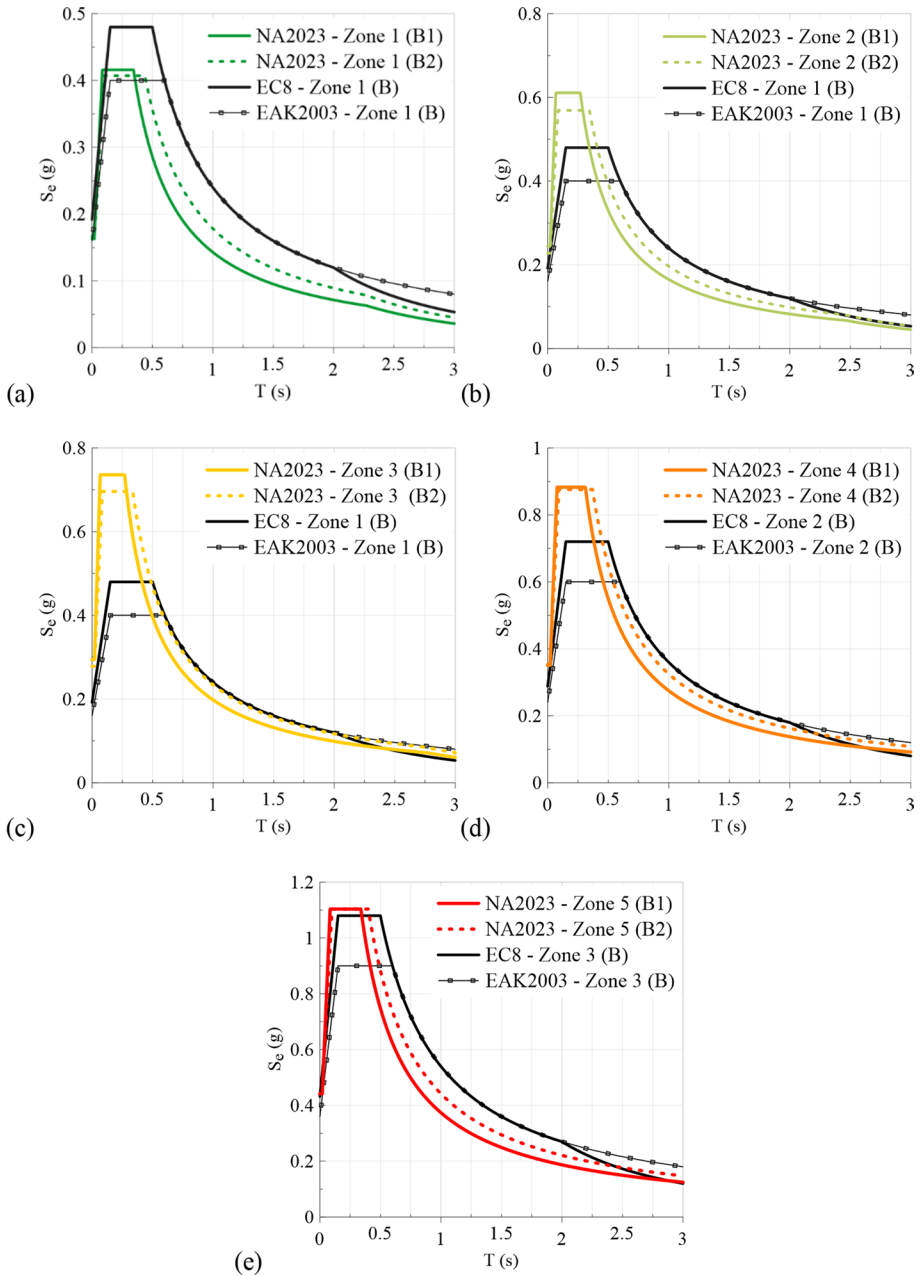


**Fig. 15** Comparison of the elastic response spectra of the proposed zonation (NA2023) for **a** Komotini (Zone 1), **b** the city center of Athens (Zone 2), **c** Thessaloniki (Zone 3), **d** Heraklion (Zone 4), and **e** Patras (Zone 5) for soil class B1 and B2 with the respective spectra of the current version of the Eurocode 8 and EAK 2003



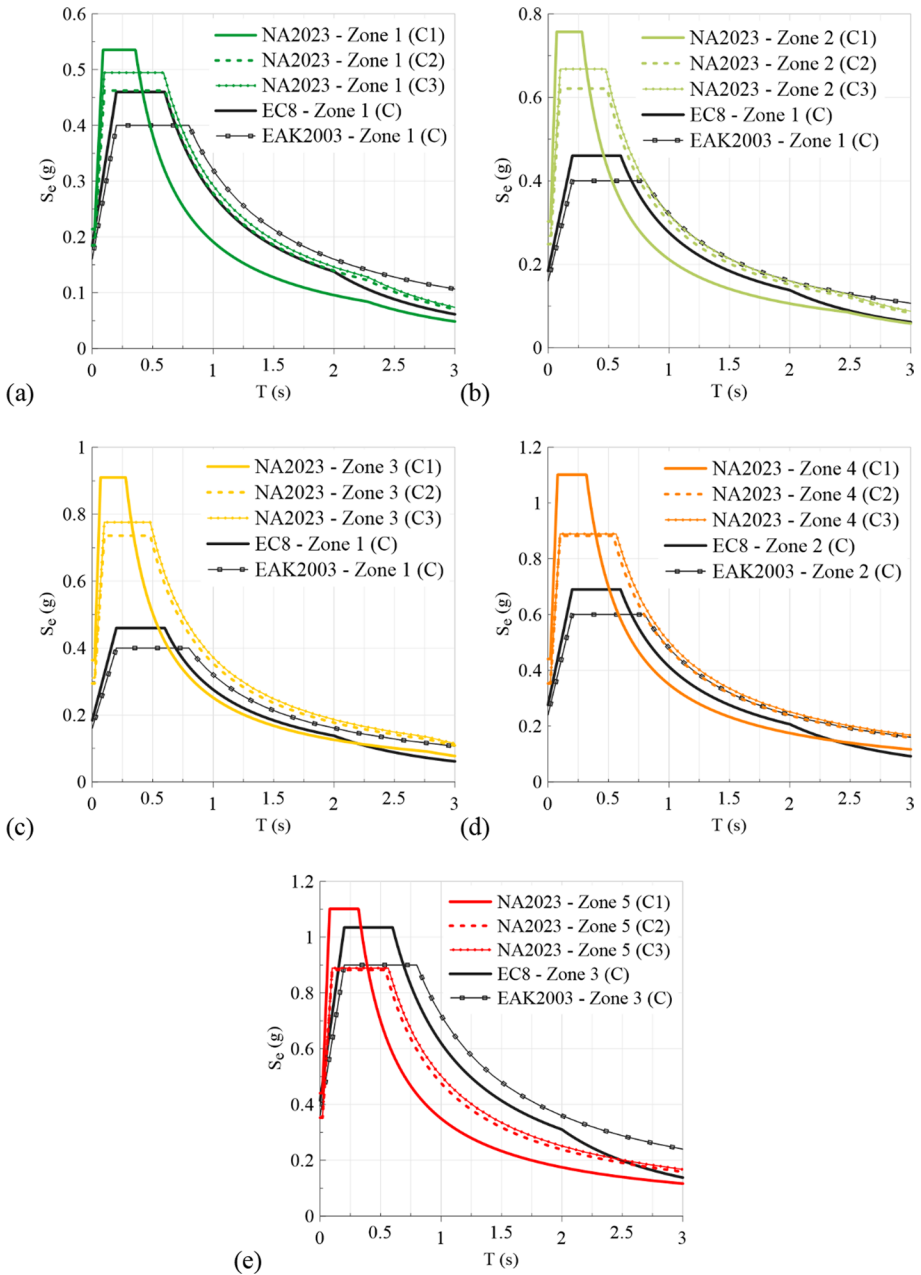


**Fig. 16** Comparison of the elastic response spectra of the proposed zonation (NA2023) for **a** Komotini (Zone 1), **b** the city center of Athens (Zone 2), **c** Thessaloniki (Zone 3), **d** Heraklion (Zone 4), and **e** Patras (Zone 5) for soil class C1, C2 and C3 with the respective spectra of the current version of the Eurocode 8 and EAK 2003

demand with NA2023 is observed for spectral periods less than 0.5–0.6 s and thus regards relatively stiff structures of medium height.

## 6 Impact on seismic risk

To further support our proposal for the new seismic zonation map and soil categorization with the associated soil amplification factors, we attempt a preliminary investigation of the potential impact of this proposal in economic terms, through a preliminary estimation of the seismic risk of the current building stock in the Greek territory in terms of economic losses. To this end we used a low-resolution exposure model of the current residential building stock of Greece developed at municipality level and we performed deterministic scenario-type seismic risk analyses with the OpenQuake-Engine considering that the current building stock of Greece is exposed to the 475y-return period ground motion as obtained from the two seismic regulations in force, i.e. EAK 2003 and current Eurocode 8, as well as the new proposal presented herein for the Greek National Annex (NA2023) in the context of the revision of EC8. Although the analysis is performed under numerous assumptions and simplifications, described in reasonable detail in the following, it provides a first-level insight into the economic impact of a potential endorsement of the herein presented proposal.

### 6.1 Development of the exposure model for the building stock of Greece

A coarse exposure model at municipality-level resolution was developed for Greece to describe the examined elements at risk, i.e., the buildings predominantly utilized for residential purposes. To this end, we classified all the residential buildings into typologies using the GED4ALL Building Taxonomy (Silva et al. 2022) shown in Table 6, which has been widely adopted by exposure models used for the risk assessment at large scale (e.g. by the Global Earthquake Model, Silva et al. 2018 and the European Seismic Risk Model ESRM20, Crowley et al. 2021). This system enables the classification of buildings based on essential structural characteristics such as the primary construction material, the lateral load resisting system, the height expressed in number of storeys, the ductility level directly related to the period of construction and the respective level of the design code. We used the data from the 2011 Population-Housing and Building Census (ELSTAT 2011), which include detailed data on the type of use, the construction material, the number of storeys, and the period of construction for the building stock of Greece in different administration levels. For the lateral load-resisting system, we made some assumptions based on the feedback from the SERA European Building Exposure Workshop questionnaire (<https://sites.google.com/eucentre.it/sera-exposureworkshop/questionnaire>). The exposure model for Greece, developed at municipality level, consists of 3,197,330 residential buildings which are classified into 161 typologies based on the GED4ALL building taxonomy. Figure 17 shows the classification of the buildings in their main structural attributes. It is worth mentioning that more than 60% of the buildings are constructed with reinforced concrete and more than 70% have been designed with low code level (DUL) or even no seismic code (DNO). Almost 80% of the buildings at country-level are low-rise (1–2 storeys), but this percentage is highly influenced by the high number of buildings located in rural areas. For example, in Thessaloniki, the second largest city of Greece almost 35% of the buildings are

**Table 6** Values of attributes of GED4ALL Building Taxonomy (Silva et al. 2022) used to describe the building stock of Greece

Attribute	Element code	Level 1 value	Element code	Level 2 value	
Material	CR	Concrete, reinforced			
	MUR	Masonry, unreinforced	CL99	Fired clay unit, unknown type	
Lateral load-resisting system (LLRS)			CB99	Concrete blocks, unknown type	
	S	Steel	STDRE	Stone	
	W	Wood			
	LFM	Moment frame			
	LFTNF	Infilled frame			
	LWAL	Walls and frames where the walls, due to their substantial lengths, resist the vast majority of the lateral load			
	LDUAL	Moment frames and shear walls acting together to resist seismic effects			
	Ductility level—Seismic code level	DNO or CDN	Non-ductile (Period of construction: before 1959)		
		DUCL or CDL	Ductile, low (Period of construction: 1960–1985)		
		DUCM or CDM	Ductile, medium (Period of construction: 1986–1995)		
DUCH or CDH		Ductile, high (Period of construction: 1996–present)			
Height	H	Exact number of storeys above ground			
Lateral force coefficient	Number expressed in %	The value of the lateral force coefficient, i.e. the fraction of the weight that was specified as the design lateral force in the seismic design code (Applied to reinforced concrete moment and infilled frames only)			

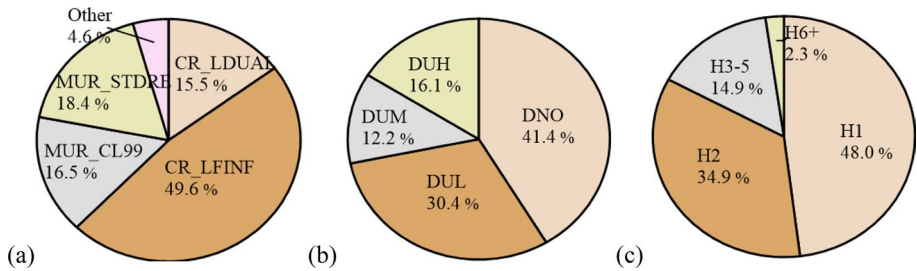


**Fig. 17** Classification of the building taxonomies in Greece 2011 based on **a** material and lateral load resisting system (LLRS), **b** code level, and **c** height according to the GED4ALL Building Taxonomy scheme of Table 5

low-rise (1–2 storeys), 50% are medium-rise (3–5 storeys) and 15% are high-rise (6+ storeys) (Riga et al. 2022).

## 6.2 Evaluation of seismic risk

For the exposure model described in the previous section, we performed scenario-type seismic risk analyses with the OpenQuake-Engine (Paganì et al. 2014; Silva et al. 2014), applying the vulnerability model by Martins and Silva (2020), employed by the Global Earthquake Model for their Global Seismic Risk Map (Silva et al. 2018). For the seismic demand we applied three different representations of the ground motion (denoted as ground motion fields in the OpenQuake-Engine), corresponding to the two seismic codes in force, i.e. EAK 2003 and the current Eurocode 8 (EC8), as well of the new proposal for the Greek National Annex of the revised EC8 (NA2023) presented in this work. EAK 2003 and current EC8 both share the same seismic hazard map (Fig. 1); however, they differ in the definition of the elastic response spectrum, with the main difference lying in the absence of soil amplification for EAK 2003. The NA2023 proposal involves the herein proposed seismic hazard map (Fig. 11) and site categorization with associated amplification factors (Tables 3 and 4).

Similarly to the resolution of the exposure model, ground motion fields for the scenario-type seismic risk analyses with the OpenQuake-Engine, i.e., PGA, Sa(0.3 s), Sa(0.6 s), and Sa(1.0 s) need to be estimated at municipality level, and more specifically at the locations of the center of each municipality, an absolutely necessary hypothesis due to the large-scale analysis, which already implies important uncertainties. The aforementioned intensity measures are the ones used in the applied vulnerability model by Martins and Silva (2020).

To account also for the effect of local site conditions, the required intensity measures need to be estimated at the ground surface. To this end, a site categorization of the study area (Greece) based on the categorization schemes of the three different codes is needed. This is practically impossible on a large scale, so the categorization should be inevitably based on very simplified models, which for example correlate  $V_{s,30}$  with topography and/or geology (e.g. Wald and Allen 2007). These models introduce high uncertainties, which should be accounted for in the discussion that will follow.

The model that we adopted in this first-order study is the ESRM20 site model (Weatherill et al. 2021; 2022), which is based on slope and geology information at European scale; consequently, we classified each municipality into site categories as recommended in EAK

2003, EC8, and the new NA2023 proposed herein. This is another rough approximation, as local site conditions are expected to vary significantly within a single municipality. Concerning the classification according to NA2023, due to the lack of adequate data on depth to seismic bedrock,  $H_B$ , for the proper classification, we assumed an intermediated depth for all cases, and thus all EC8 soil type B sites were classified as B2, while all EC8 soil type C sites were classified as C2. Finally, for the sites corresponding to the centers of each municipality, we calculated the 475-year return period elastic response spectra according to (a) EAK 2003, (b) EC8 and (c) NA2023 (as was described also in Sect. 5) and extracted from them the PGA, and spectral accelerations  $S_a(0.3\text{ s})$ ,  $S_a(0.6\text{ s})$ , and  $S_a(1.0\text{ s})$ . These values constitute the ground motion fields that were used in the scenario risk analyses at municipality scale.

The combination of the exposure model, the ground motion fields and the vulnerability model provides for the three seismic codes the estimated loss ratio, i.e. the ratio of the repair cost to the replacement cost, for each element of the exposure model (i.e., the buildings of each taxonomy per municipality), as well as the aggregate loss ratio for the total building portfolio of the residential buildings at municipality level (Fig. 18). The general outcome is that for most municipalities EAK 2003 leads to lower loss ratio values (Fig. 18a), which is expected and explained mainly by the fact that soil amplification is neglected, leading to lower seismic demand and therefore to lower seismic risk. On the

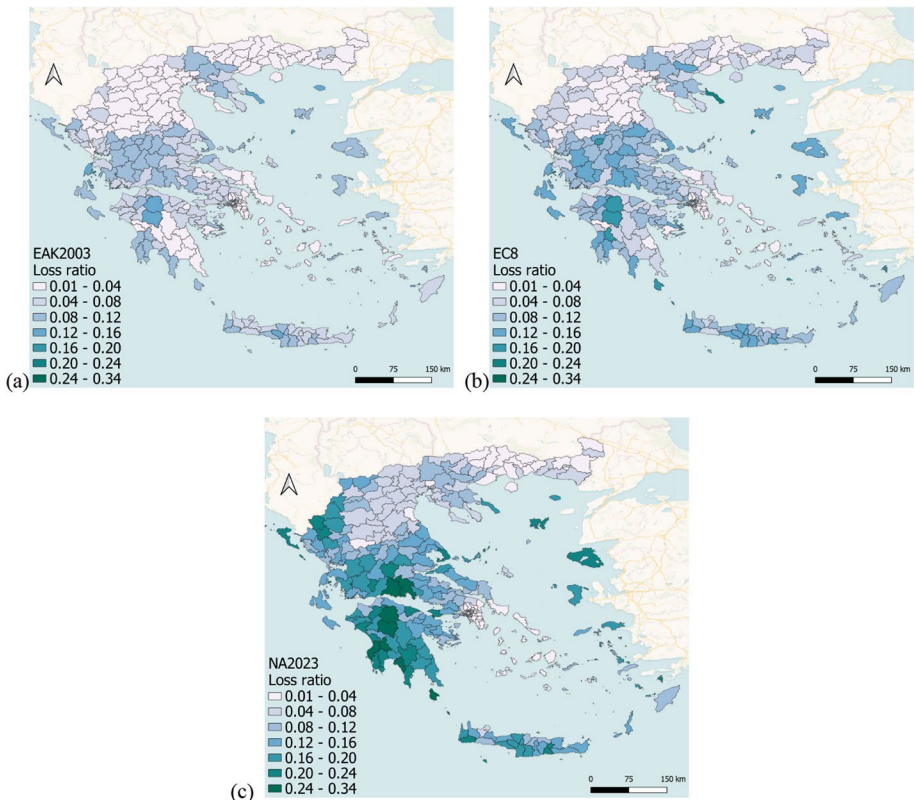


**Fig. 18** Loss ratio maps at municipality level for Greece considering **a** EAK 2003, **b** EC8, and **c** NA2023



other hand, the new NA2023 proposal in most cases results in higher seismic demand and seismic risk (Fig. 18c), due to both the higher soil amplification factors, which is perfectly justified, and the higher ground shaking hazard for rock conditions in some parts of the country. The current Eurocode 8 results in intermediate loss ratios (Fig. 18b). However, there is a significant number of municipalities (around 90 out of the total 326) where the estimated loss ratios with NA2023 are lower than the ones of EC8, such as specific municipalities in Attica, Central Macedonia and Thrace. For EAK 2003 the highest loss ratios are observed in Central Greece, the Ionian islands, Central Macedonia, in certain municipalities in Peloponnese around the Corinthian Gulf, in Crete, and the eastern Aegean islands, with loss ratios between 8 and 16% (Fig. 18a), while for Eurocode 8 they range between 12 and 24% (Fig. 18b). Indeed, as shown in Fig. 19, the normal distribution curve of the loss ratio values for the current EC8 is shifted slightly to the right compared to EAK 2003. For the herein proposed NA2023, almost 25% of the municipalities and 20% of the total building portfolio, mainly in Zones 4 and 5, exhibit loss ratio values higher than 16% (Fig. 18c). On the contrary, regions located in Zone 1 (Thrace and the islands of Cyclades) show low loss ratio values below 8%, whereas the remaining municipalities, located in Zones 2 and 3, cover all the intermediate values of the histogram in Fig. 19. Regarding the 61 selected cities, the highest loss ratios with NA2023 (above 20%) are found in Amfissa, Limnos, Mytilini, Pyrgos, Sparti and Kerkyra (Corfu), which anyway should be expected, while the lowest (below 5%) are located in Katerini, Trikala, Kavala, Santorini, Drama and Xanthi.

Moving to national level, we made unavoidable assumptions for the replacement cost per area (1500 €/m<sup>2</sup> for Athens and Thessaloniki and 1200 €/m<sup>2</sup> for the rest municipalities of Greece) and for the floor area (90 m<sup>2</sup> for low-rise buildings (1–2 storeys) and 300 m<sup>2</sup> for the rest height categories), to make a broad estimation of the aggregated loss ratio and economic losses at country level for the 475 year return period (Table 7). This offers an indication of the impact of the adopted code on the estimated risk at national scale. In line with the previous observations, EAK 2003 leads to the lowest aggregated risk (i.e., 28 billion €), while the new NA2023 proposal results in a reasonable increase of the estimated aggregated risk (49 billion €) compared to the current EC8 (36 billion €), with which it should be directly compared. One should keep in mind, however, that for a significant number of

**Fig. 19** Histograms and normal distribution curves for the calculated loss ratio values over the municipalities of Greece

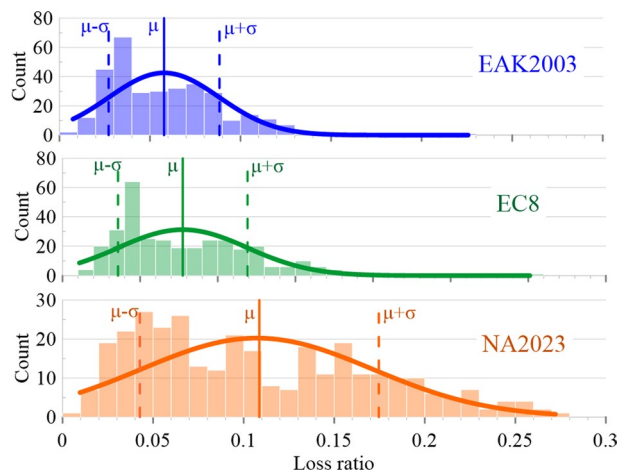


**Table 7** Aggregated economic losses and loss ratios for Greece obtained from the scenario risk analyses

Hazard model	Loss ratio	Economic losses (billion €)
EAK2003	0.055	27.96
EC8	0.071	36.27
NA2023	0.097	49.19

municipalities a decrease in risk is observed with the adoption on NA2023. The aggregated economic losses estimated with the NA2023 are quite close to the  $47.4 \pm 6.6$  billion € estimated by Silva et al. (2015) for 475-year return period for mainland Portugal, a country with similar number of buildings. Last but not least, the results of these risk analyses should be treated with caution due to the numerous uncertainties involved, with respect to the resolution of the exposure model and the seismic demand, the site modelling, as well as the adopted vulnerability models. In any case, they should be considered only as supporting material for the proposed zonation.

## 7 Conclusions

In the context of the ongoing revision of Part 1 of Eurocode 8, we present a complete proposal for the definition of seismic actions for potential adoption by the Greek National Annex of the new version of Eurocode 8—Part 1, consisting primarily of a new seismic hazard zonation map and of a novel site categorization scheme, as well as of all the necessary parameters for the definition of the elastic response spectra. The proposed ground shaking zonation map was developed mainly based on the 2020 European Seismic Hazard Model (ESHM20, Danciu et al. 2021; 2022; 2024). In addition, population and administrative criteria were also adopted, for the fine-tuning of the boundaries of the zones. The map comprises five seismic zones compared to the three zones of the seismic hazard map in force. The lowest seismic zones (1 and 2) contain Thrace (except for the city of Alexandroupoli), the eastern part of Attica, the islands of Cyclades, the greatest part of central and western Macedonia, northern Thessaly as well as the central part of Attica. The highest seismic hazard zones (4 and 5) include western Greece and the Ionian islands, the greatest part of central Greece and Peloponnese (including the Corinthian Gulf), Crete and the island of eastern Aegean. The map is consistent with the well-known and documented seismic history in Greece, while it considers the importance of the population density and the general importance of the regions. In the proposal presented herein, it has been decided for consistency reasons to keep the zonation and the respective PGA,  $S_{\alpha,475}$  and  $S_{\beta,475}$  values for each zone as they have been calculated from the adopted methodology. However, in the case of a potential official adoption of the map by the Greek National Annex of the new Eurocode 8, some practical adjustments might need to be considered, such as rounding the proposed  $S_{\alpha,475}$ ,  $S_{\beta,475}$ ,  $F_{\alpha}$  and  $F_{\beta}$  values of the zones, increasing the hazard level of Zone 1, or homogenization of the Athens region in two zones instead of three, to ensure consensus and an easier application by the practitioners.

Regarding site classification, the proposed scheme is based on previous efforts of the authors and introduces the approximate depth to seismic bedrock as the main classification parameter in addition to equivalent shear wave velocity and fundamental period of the site.

For each class and each seismic zone, appropriate intensity-dependent site amplification factors are provided, accounting also for nonlinear site response.

The proposal is supported by a preliminary investigation of the impact of its potential adoption on the seismic design and risk of the building stock in Greece, to help gain a better insight on how important the imposed differences might be for the end-users and the administration. Regarding the elastic response spectra used for the seismic design, the adoption of the proposal may result in some cases, in an increase of the seismic demand due to the increased hazard for rock conditions as well as the higher site amplification factors, which is however limited at spectral periods less than 0.5–0.6 s and thus regards relatively stiff structures of medium height. On the contrary, for the low hazard Zones 1 and 2 the maximum spectral acceleration may decrease compared to the current codes, depending on the soil conditions. This is something that will possibly need to be discussed by the relevant authorities in charge of the National Annex. The discrepancies are more pronounced with respect to EAK 2003 due to the complete absence of site amplification in this code. With respect to the impact of our proposal on the seismic risk, the preliminary analyses showed that a reasonable increase is expected at the estimated risk at national level, justified by the increase in the seismic demand in a significant number of municipalities. These results, however, should be treated with caution due to the numerous uncertainties involved, with respect to the resolution of the exposure model and the seismic demand, the site modelling, as well as the adopted vulnerability models.

## Appendix

See Table 8, 9 and 10.

**Table 8**  $(PGA_{zone}-PGA_{point})/PGA_{point}$  ratios for 61 cities in Greece (Fig. 4) in ascending order for the three-zone seismic hazard map of Fig. 8a

City	ESHM20: PGA <sub>point</sub> (g)	Zone	PGA <sub>zone</sub> (g)	(PGA <sub>zone</sub> - PGA <sub>point</sub> ) (g)	(PGA <sub>zone</sub> - PGA <sub>point</sub> ) / PGA <sub>point</sub>	Population	Thresh- old satis- fied
Santorini	0.22	1	0.15	-0.07	-31.82%	15,550	No
Aigio	0.47	3	0.33	-0.14	-29.79%	20,442	No
Argostoli	0.44	3	0.33	-0.11	-25.00%	9,748	No
Nafpaktos	0.44	3	0.33	-0.11	-25.00%	13,415	No
Lefkada	0.42	3	0.33	-0.09	-21.43%	8,673	No
Zakynthos	0.4	3	0.33	-0.07	-17.50%	9,772	Yes
Preveza	0.4	3	0.33	-0.07	-17.50%	19,042	Yes
Edessa	0.18	1	0.15	-0.03	-16.67%	18,229	Yes
Veroia	0.18	1	0.15	-0.03	-16.67%	43,158	Yes
Katerini	0.18	1	0.15	-0.03	-16.67%	55,997	Yes
Almyros	0.28	2	0.24	-0.04	-14.29%	7,955	Yes
Agrinio	0.28	2	0.24	-0.04	-14.29%	55,097	Yes
Chalkida	0.28	2	0.24	-0.04	-14.29%	59,125	Yes
Tripoli	0.28	2	0.24	-0.04	-14.29%	30,866	Yes
Skopelos	0.28	2	0.24	-0.04	-14.29%	3,090	Yes
Patras	0.38	3	0.33	-0.05	-13.16%	168,202	Yes
Alexandroupoli	0.17	1	0.15	-0.02	-11.76%	57,812	Yes
Serres	0.17	1	0.15	-0.02	-11.76%	58,287	Yes
Arta	0.27	2	0.24	-0.03	-11.11%	21,895	Yes
Kerkyra	0.27	2	0.24	-0.03	-11.11%	24,838	Yes
Volos	0.27	2	0.24	-0.03	-11.11%	118,707	Yes
Karpenisi	0.26	2	0.24	-0.02	-7.69%	7,183	Yes
Lamia	0.26	2	0.24	-0.02	-7.69%	52,066	Yes
Mesologgi	0.26	2	0.24	-0.02	-7.69%	12,785	Yes
Kalamata	0.35	3	0.33	-0.02	-5.71%	54,100	Yes
Pyrgos	0.35	3	0.33	-0.02	-5.71%	24,359	Yes
Nafplion	0.25	2	0.24	-0.01	-4.00%	14,203	Yes
Athos	0.25	2	0.24	-0.01	-4.00%	2,072	Yes
Korinthos	0.34	3	0.33	-0.01	-2.94%	30,176	Yes
Amfissa	0.33	3	0.33	0	0.00%	6,919	Yes
Drama	0.15	1	0.15	0	0.00%	54,027	Yes
Samos	0.33	3	0.33	0	0.00%	8,079	Yes
Limnos	0.24	2	0.24	0	0.00%	49,541	Yes
Rhodes	0.33	3	0.33	0	0.00%	49,541	Yes
Sparti	0.33	3	0.33	0	0.00%	18,926	Yes
Ioannina	0.32	3	0.33	0.01	3.13%	65,574	Yes
Polygyros	0.23	2	0.24	0.01	4.35%	6,121	Yes
Thessaloniki	0.23	2	0.24	0.01	4.35%	789,191	Yes
Karditsa	0.23	2	0.24	0.01	4.35%	38,554	Yes
Kastoria	0.23	2	0.24	0.01	4.35%	13,387	Yes
Heraklion	0.31	3	0.33	0.02	6.45%	163,653	Yes
Agios Nicolaos	0.31	3	0.33	0.02	6.45%	11,421	Yes

**Table 8** (continued)

City	ESHM20: PGA <sub>point</sub> (g)	Zone	PGA <sub>zone</sub> (g)	(PGA <sub>zone</sub> - PGA <sub>point</sub> ) (g)	(PGA <sub>zone</sub> - PGA <sub>point</sub> ) / PGA <sub>point</sub>	Population	Thresh- old satis- fied
Thiva	0.31	3	0.33	0.02	6.45%	22,883	Yes
Rethymno	0.31	3	0.33	0.02	6.45%	32,468	Yes
Florina	0.22	2	0.24	0.02	9.09%	17,686	Yes
Chios	0.3	3	0.33	0.03	10.00%	26,850	Yes
Kos	0.3	3	0.33	0.03	10.00%	19,432	Yes
Mytilini	0.29	3	0.33	0.04	13.79%	27,871	Yes
Chania	0.29	3	0.33	0.04	13.79%	53,910	Yes
Athens	0.21	2	0.24	0.03	14.29%	3,218,218	No
Kilkis	0.21	2	0.24	0.03	14.29%	22,914	Yes
Grevena	0.21	2	0.24	0.03	14.29%	13,137	Yes
Larissa	0.21	2	0.24	0.03	14.29%	144,651	Yes
Komotini	0.13	1	0.15	0.02	15.38%	50,990	Yes
Xanthi	0.13	1	0.15	0.02	15.38%	56,122	Yes
Kozani	0.2	2	0.24	0.04	20.00%	41,066	Yes
Ptolemaida	0.2	2	0.24	0.04	20.00%	32,142	Yes
Igoumenitsa	0.27	3	0.33	0.06	22.22%	9,145	No
Kavala	0.12	1	0.15	0.03	25.00%	54,027	No
Trikala	0.19	2	0.24	0.05	26.32%	61,653	No

Negative or positive values of the ratio mean that the zonation of Fig. 8a underestimates or overestimates PGA with respect to the closest grid point, respectively

**Table 9**  $(PGA_{zone} - PGA_{point})/PGA_{point}$  ratios for 61 cities in Greece (Fig. 4) in ascending order for the four-zone seismic hazard map of Fig. 9a

City	ESHM20: PGA <sub>point</sub> (g)	Zone	PGA <sub>zone</sub> (g)	(PGA <sub>zone</sub> - PGA <sub>point</sub> ) (g)	(PGA <sub>zone</sub> - PGA <sub>point</sub> ) / PGA <sub>point</sub>	Population	Thresh- old satisfied
Alexandroupoli	0.17	1	0.12	-0.05	-29.41%	57,812	No
Aigio	0.47	4	0.37	-0.1	-21.28%	20,442	No
Athos	0.25	2	0.2	-0.05	-20.00%	2,072	Yes
Drama	0.15	1	0.12	-0.03	-20.00%	54,027	Yes
Argostoli	0.44	4	0.37	-0.07	-15.91%	9,748	Yes
Nafpaktos	0.44	4	0.37	-0.07	-15.91%	13,415	Yes
Samos	0.33	3	0.28	-0.05	-15.15%	8,079	Yes
Rhodes	0.33	3	0.28	-0.05	-15.15%	49,541	Yes
Sparti	0.33	3	0.28	-0.05	-15.15%	18,926	Yes
Polygyros	0.23	2	0.2	-0.03	-13.04%	6,121	Yes
Thessaloniki	0.23	2	0.2	-0.03	-13.04%	789,191	No
Kastoria	0.23	2	0.2	-0.03	-13.04%	13,387	Yes
Ioannina	0.32	3	0.28	-0.04	-12.50%	65,574	Yes
Lefkada	0.42	4	0.37	-0.05	-11.90%	8,673	Yes
Heraklion	0.31	3	0.28	-0.03	-9.68%	163,653	Yes
Agios Nicolaos	0.31	3	0.28	-0.03	-9.68%	11,421	Yes
Thiva	0.31	3	0.28	-0.03	-9.68%	22,883	Yes
Rethymno	0.31	3	0.28	-0.03	-9.68%	32,468	Yes
Santorini	0.22	2	0.2	-0.02	-9.09%	15,550	Yes
Florina	0.22	2	0.2	-0.02	-9.09%	17,686	Yes
Komotini	0.13	1	0.12	-0.01	-7.69%	50,990	Yes
Xanthi	0.13	1	0.12	-0.01	-7.69%	56,122	Yes
Zakynthos	0.4	4	0.37	-0.03	-7.50%	9,772	Yes
Preveza	0.4	4	0.37	-0.03	-7.50%	19,042	Yes
Chios	0.3	3	0.28	-0.02	-6.67%	26,850	Yes
Kos	0.3	3	0.28	-0.02	-6.67%	19,432	Yes
Athens	0.21	2	0.2	-0.01	-4.76%	3,218,218	Yes
Kilkis	0.21	2	0.2	-0.01	-4.76%	22,914	Yes
Grevena	0.21	2	0.2	-0.01	-4.76%	13,137	Yes
Mytilini	0.29	3	0.28	-0.01	-3.45%	27,871	Yes
Chania	0.29	3	0.28	-0.01	-3.45%	53,910	Yes
Patras	0.38	4	0.37	-0.01	-2.63%	168,202	Yes
Almyros	0.28	3	0.28	0	0.00%	7,955	Yes
Agrinio	0.28	3	0.28	0	0.00%	55,097	Yes
Chalkida	0.28	3	0.28	0	0.00%	59,125	Yes
Tripoli	0.28	3	0.28	0	0.00%	30,866	Yes
Skopelos	0.28	3	0.28	0	0.00%	3,090	Yes
Kozani	0.2	2	0.2	0	0.00%	41,066	Yes
Ptolemaida	0.2	2	0.2	0	0.00%	32,142	Yes
Kavala	0.12	1	0.12	0	0.00%	54,027	Yes
Arta	0.27	3	0.28	0.01	3.70%	21,895	Yes
Kerkyra	0.27	3	0.28	0.01	3.70%	24,838	Yes

**Table 9** (continued)

City	ESHM20: PGA <sub>point</sub> (g)	Zone	PGA <sub>zone</sub> (g)	(PGA- zone - PGA <sub>point</sub> ) (g)	(PGA- zone - PGA <sub>point</sub> ) / PGA <sub>point</sub>	Population	Thresh- old satisfied
Volos	0.27	3	0.28	0.01	3.70%	118,707	Yes
Igoumenitsa	0.27	3	0.28	0.01	3.70%	9,145	Yes
Trikala	0.19	2	0.2	0.01	5.26%	61,653	Yes
Kalamata	0.35	4	0.37	0.02	5.71%	54,100	Yes
Pyrgos	0.35	4	0.37	0.02	5.71%	24,359	Yes
Karpenisi	0.26	3	0.28	0.02	7.69%	7,183	Yes
Lamia	0.26	3	0.28	0.02	7.69%	52,066	Yes
Mesologgi	0.26	3	0.28	0.02	7.69%	12,785	Yes
Korinthos	0.34	4	0.37	0.03	8.82%	30,176	Yes
Edessa	0.18	2	0.2	0.02	11.11%	18,229	Yes
Veroia	0.18	2	0.2	0.02	11.11%	43,158	Yes
Katerini	0.18	2	0.2	0.02	11.11%	55,997	Yes
Nafplion	0.25	3	0.28	0.03	12.00%	14,203	Yes
Amfissa	0.33	4	0.37	0.04	12.12%	6,919	Yes
Limnos	0.24	3	0.28	0.04	16.67%	49,541	Yes
Serres	0.17	2	0.2	0.03	17.65%	58,287	Yes
Karditsa	0.23	3	0.28	0.05	21.74%	38,554	No
Larissa	0.21	3	0.28	0.07	33.33%	144,651	No

Negative or positive values of the ratio mean that the zonation of Fig. 9a underestimates or overestimates PGA with respect to the closest grid point, respectively



**Table 10**  $(PGA_{zone} - PGA_{point})/PGA_{point}$  ratios for 61 cities in Greece (Fig. 4) in ascending order for the five-zone seismic hazard map of Fig. 10a

City	ESHM20: $PGA_{point}$ (g)	Zone	$PGA_{zone}$ (g)	$(PGA_{zone} - PGA_{point})$ (g)	$(PGA_{zone} - PGA_{point})$ $/ PGA_{point}$	Population	Thresh- old satisfied
Aigio	0.46	5	0.37	-0.09	-19.57%	20,442	Yes
Argostoli	0.44	5	0.37	-0.07	-15.91%	9,748	Yes
Nafpaktos	0.44	5	0.37	-0.07	-15.91%	13,415	Yes
Santorini	0.22	2	0.19	-0.03	-13.64%	15,550	Yes
Drama	0.15	1	0.13	-0.02	-13.33%	54,027	Yes
Samos	0.33	4	0.29	-0.04	-12.12%	8,079	Yes
Rhodes	0.33	4	0.29	-0.04	-12.12%	49,541	Yes
Sparti	0.33	4	0.29	-0.04	-12.12%	18,926	Yes
Lefkada	0.42	5	0.37	-0.05	-11.90%	8,673	Yes
Athens	0.21	2	0.19	-0.02	-9.52%	3,218,218	Yes
Kilkis	0.21	2	0.19	-0.02	-9.52%	22,914	Yes
Grevena	0.21	2	0.19	-0.02	-9.52%	13,137	Yes
Ioannina	0.32	4	0.29	-0.03	-9.38%	65,574	Yes
Athos	0.25	3	0.23	-0.02	-8.00%	2,072	Yes
Zkyntos	0.4	5	0.37	-0.03	-7.50%	9,772	Yes
Preveza	0.4	5	0.37	-0.03	-7.50%	19,042	Yes
Heraklion	0.31	4	0.29	-0.02	-6.45%	163,653	Yes
Agios Nicolaos	0.31	4	0.29	-0.02	-6.45%	11,421	Yes
Thiva	0.31	4	0.29	-0.02	-6.45%	22,883	Yes
Rethymno	0.31	4	0.29	-0.02	-6.45%	32,468	Yes
Kozani	0.2	2	0.19	-0.01	-5.00%	41,066	Yes
Ptolemaida	0.2	2	0.19	-0.01	-5.00%	32,142	Yes
Chios	0.3	4	0.29	-0.01	-3.33%	26,850	Yes
Kos	0.3	4	0.29	-0.01	-3.33%	19,432	Yes
Patras	0.38	5	0.37	-0.01	-2.63%	168,202	Yes
Polygyros	0.23	3	0.23	0	0.00%	6,121	Yes
Thessaloniki	0.23	3	0.23	0	0.00%	789,191	Yes
Kastoria	0.23	3	0.23	0	0.00%	13,387	Yes
Komotini	0.13	1	0.13	0	0.00%	50,990	Yes
Xanthi	0.13	1	0.13	0	0.00%	56,122	Yes
Mytilini	0.29	4	0.29	0	0.00%	27,871	Yes
Chania	0.29	4	0.29	0	0.00%	53,910	Yes
Trikala	0.19	2	0.19	0	0.00%	61,653	Yes
Karditsa	0.23	3	0.23	0	0.00%	38,554	Yes
Almyros	0.28	4	0.29	0.01	3.57%	7,955	Yes
Agrinio	0.28	4	0.29	0.01	3.57%	55,097	Yes
Chalkida	0.28	4	0.29	0.01	3.57%	59,125	Yes
Tripoli	0.28	4	0.29	0.01	3.57%	30,866	Yes
Skopelos	0.28	4	0.29	0.01	3.57%	3,090	Yes
Florina	0.22	3	0.23	0.01	4.55%	17,686	Yes
Edessa	0.18	2	0.19	0.01	5.56%	18,229	Yes
Veroia	0.18	2	0.19	0.01	5.56%	43,158	Yes

**Table 10** (continued)

City	ESHM20: PGA <sub>point</sub> (g)	Zone	PGA <sub>zone</sub> (g)	(PGA- zone - PGA <sub>point</sub> ) (g)	(PGA- zone - PGA <sub>point</sub> ) / PGA <sub>point</sub>	Population	Thresh- old satisfied
Katerini	0.18	2	0.19	0.01	5.56%	55,997	Yes
Kalamata	0.35	5	0.37	0.02	5.71%	54,100	Yes
Pyrgos	0.35	5	0.37	0.02	5.71%	24,359	Yes
Arta	0.27	4	0.29	0.02	7.41%	21,895	Yes
Kerkyra	0.27	4	0.29	0.02	7.41%	24,838	Yes
Volos	0.27	4	0.29	0.02	7.41%	118,707	Yes
Igoumenitsa	0.27	4	0.29	0.02	7.41%	9,145	Yes
Kavala	0.12	1	0.13	0.01	8.33%	54,027	Yes
Korinthos	0.34	5	0.37	0.03	8.82%	30,176	Yes
Larissa	0.21	3	0.23	0.02	9.52%	144,651	Yes
Karpenisi	0.26	4	0.29	0.03	11.54%	7,183	Yes
Lamia	0.26	4	0.29	0.03	11.54%	52,066	Yes
Mesologgi	0.26	4	0.29	0.03	11.54%	12,785	Yes
Alexandroupoli	0.17	2	0.19	0.02	11.76%	57,812	Yes
Serres	0.17	2	0.19	0.02	11.76%	58,287	Yes
Amfissa	0.33	5	0.37	0.04	12.12%	6,919	Yes
Nafplion	0.25	4	0.29	0.04	16.00%	14,203	Yes
Limnos	0.25	4	0.29	0.04	17.89%	49,541	Yes

Negative or positive values of the ratio mean that the zonation of Fig. 10a underestimates or overestimates PGA with respect to the closest grid point, respectively

**Acknowledgements** The authors would like to thank two anonymous reviewers for their valuable comments, effort and time allocated to improve the paper.

**Author contributions** All authors contributed during the preparation of this work and consent to publish it. KP: Conceptualization, Writing—Review & Editing, Supervision. ER: Conceptualization, Investigation, Visualization, Writing—Review & Editing. SA: Conceptualization, Investigation, Visualization, Writing—Review & Editing. LD: Review & Editing.

**Funding** Open access funding provided by HEAL-Link Greece. This research was performed without any funding or grants from any institutions or individuals.

**Data availability** OpenQuake Engine is available for download at <https://www.globalquakemodel.org/oq-get-started>. The main datasets and OpenQuake input files of ESHM20 and ESRM20 are online available at <https://gitlab.seismo.ethz.ch/efehr>. The results of the ESHM20 are open to access and download at hazard.efehr.org, whereas those of the ESRM20 are distributed by risk.efehr.org.

**Code availability** Not applicable (commercial software has been used).

## Declarations

**Conflict of interest** The authors have no conflicts of interest to declare that are relevant to the content of this article.

**Open Access** This article is licensed under a Creative Commons Attribution 4.0 International License, which permits use, sharing, adaptation, distribution and reproduction in any medium or format, as long as you give appropriate credit to the original author(s) and the source, provide a link to the Creative Commons

licence, and indicate if changes were made. The images or other third party material in this article are included in the article's Creative Commons licence, unless indicated otherwise in a credit line to the material. If material is not included in the article's Creative Commons licence and your intended use is not permitted by statutory regulation or exceeds the permitted use, you will need to obtain permission directly from the copyright holder. To view a copy of this licence, visit <http://creativecommons.org/licenses/by/4.0/>.

## References

- Abrahamson N, Gregor N, Addo K (2016) BC hydro ground motion prediction equations for subduction earthquakes. *Earthq Spectra* 32(1):23–44. <https://doi.org/10.1193/051712EQS188M>
- Akkar S, Azak T, Çan T, Çeken U, Demircioğlu MB, Duman T, Ergintav S, Kadirioğlu FT, Kalafat D, Kale Ö, Kartal R F, Kılıç T, Özalp S, Altuncu S P, Şeşetyan K, Tekin S, Yakut A., Yılmaz M T, Yüçemen MS, Zülfikar Ö (2007) Updated Probabilistic Seismic Hazard Maps for Turkey.
- Anagnostopoulos A, Koukis G, Sabatakakis N, Tsiambaos G (2003) Empirical correlations of soil parameters based on cone penetration tests (CPT) for Greek soils. *Geotech Geol Eng* 21:377–387
- Athanasopoulos G (1994) Empirical correlation  $V_s$ –NSPT for soils of Greece. In: *Proceedings of the 2nd International Conference on Resistant Construction and Design, ERCAD 94*, pp 219–226, Berlin
- Basili R, Kastelic V, Demircioglu MB, Garcia Moreno D, Nemser ES, Petricca P et al (2013) The european database of seismogenic faults (EDSF) compiled in the framework of the Project SHARE. *Ist Naz Di Geo e Vulcanol (INGV)*. <https://doi.org/10.6092/INGV.IT-SHARE-EDSF>
- Basili R, Danciu L, Carafa MMC, Kastelic V, Maesano F E, Tiberti MM, Vallone R, R Gracia E, Seseştyan K, Atanackov J, Sket-Motnikar B, Zupančič P, Vanneste K, Vilanova S (2020) Insights on the European Fault-Source Model (EFSM20) as input to the 2020 update of the European Seismic Hazard Model (ESHM20). <https://doi.org/10.5194/egusphere-egu2020-7008>
- Caputo R and Pavlides S (2013) The Greek Database of Seismogenic Sources (GreDaSS), version 2.0.0: A compilation of potential seismogenic sources ( $M_w > 5.5$ ) in the Aegean Region. <http://gredass.unife.it/>, doi: <https://doi.org/10.15160/unife/gredass/0200>
- Crowley H, Dabbeek J, Despotaki V, Rodrigues D, Martins L, Silva V, Romão, X, Pereira N, Weatherill G and Danciu L (2021) European Seismic Risk Model (ESRM20), EFEHR Technical Report 002, V1.0.0, 84 pp. <https://doi.org/10.7414/EUC-EFEHR-TR002-ESRM20>
- Danciu L, Nandan S, Reyes C, Basili R, Weatherill G, Beauval C, Rovida A, Vilanova S, Sesetyan K, Bard PY, Cotton F, Wiemer S, Giardini D (2021) The 2020 update of the European Seismic Hazard Model: Model Overview. EFEHR Technical Report 001, v1.0.0, <https://doi.org/10.12686/a15>
- Danciu L, Weatherill G, Rovida A, Basili R, Bard PY, Beauval C, Nandan S, Pagani M, Crowley H, Seseştyan K, Vilanova S, Reyes C, Marti M, Cotton F, Wiemer S, Giardini D (2022). The 2020 European Seismic Hazard Model: Milestones and Lessons Learned. In: Vacareanu, R., Ionescu, C. (eds) *Progresses in European Earthquake Engineering and Seismology*. ECEES 2022. Springer Proceedings in Earth and Environmental Sciences. Springer, Cham. [https://doi.org/10.1007/978-3-031-15104-0\\_1](https://doi.org/10.1007/978-3-031-15104-0_1)
- Danciu L, Giardini D, Weatherill G, Basili R, Nandan S, Rovida A, Beauval C, Bard PY, Pagani M, Reyes CG, Sesetyan K, Vilanova S, Cotton F, Wiemer S (2024) The 2020 European seismic hazard model: overview and results, EGU sphere [preprint], <https://doi.org/10.5194/egusphere-2023-3062>
- Douglas J (2018) Calibrating the backbone approach for the development of earthquake ground motion models. *Best Practice in Physics-Based Fault Rupture Models for Seismic Hazard Assessment of Nuclear Installations: Issues and Challenges Towards Full Seismic Risk Analysis*, CEA Cadarache-Château, France.
- EAK (2003) Modification of the provisions of the Greek seismic code EAK 2000 (in Greek), Earthquake Planning and Protection Organization.
- ELSTAT (2011) Population-housing census, Hellenic Statistical Authority
- EN 1998–1 (2004) Eurocode 8: Design of structures for earthquake resistance, Part 1: General rules, seismic actions and rules for buildings, European Standard, European Committee for Standardization, Brussels, Belgium
- FEMA P-1050-1/2015 Edition. (2015). NEHRP Recommended seismic provisions for new buildings and other structures. Building Seismic Safety Council, I, 515
- Ganas A, Elias P, Briole P, Valkaniotis S, Escartin J, Tsironi V, Karasante I, Kosma C (2021) Co-seismic and post-seismic deformation, field observations and fault model of the 30 October 2020  $M_w = 7.0$  Samos earthquake. *Aegean Sea Acta Geophys* 69:999–1024. <https://doi.org/10.1007/s11600-021-00599-1>

- Giardini D, Woessner J, Danciu L, Valensise G, Arvidsson R, Sesetyan K, et al (2013) Seismic Hazard Harmonization in Europe (SHARE): Online Data Resource, doi: <https://doi.org/10.12686/SED-00000-001-SHARE>
- Grünthal G, Wahlström R (2012) The European-Mediterranean earthquake catalogue (EMEC) for the last millennium. *J Seismol* 16(3):535–570
- Idriss I, Boulanger R (2007) SPT- and CPT-based relationships for the residual shear strength of liquefied soils. In: Pitolakis K (ed) earthquake geotechnical engineering, 4th international conference on earthquake geotechnical engineering-invited lectures Geotechnical, Geological and Earthquake Engineering, vol 6. Springer, Netherlands, pp 1–22
- Haslinger F, Basili R, Bossu R, Cauzzi C, Cotton F, Crowley H, Custodio S, Danciu L, Locati M, Michelini A, Molinari I, Ottemöller L, Parolai S (2022) Coordinated and interoperable seismological data and product services in Europe: The EPOS thematic core service for seismology. *Annals of Geophysics*, doi: <https://doi.org/10.4401/ag-8767>
- Jenks GF (1967) The Data model concept in statistical mapping. *International Yearbook of Cartography* 7:186–190
- Kotha SR, Weatherill G, Cotton F (2020) A regionally adaptable ground-motion model for shallow crustal earthquakes in Europe. *Bull Earthq Eng* 18:4091–4125
- Kotha Sreeram Reddy, Weatherill Graeme, Bindi Dino, Cotton Fabrice (2022) Near-source magnitude scaling of spectral accelerations: analysis and update of Kotha et al. (2020) model. *Bull Earthq Eng* 20(3):1343–1370. <https://doi.org/10.1007/s10518-021-01308-5>
- Lanzano G, Puglia R, Russo E, Luzi L, Bindi D, Cotton F, D'Amico M, Felicetta C, Pacor F & ORFEUS WG5 (2018) ESM strong-motion flat-file 2018. Istituto Nazionale di Geofisica e Vulcanologia (INGV), Helmholtz-Zentrum Potsdam Deutsches GeoForschungsZentrum (GFZ), Observatories & Research Facilities for European Seismology (ORFEUS). PID: 11099/ESM\_flatfile\_2018
- Labbé Pierre, Paolucci Roberto (2022) Developments relating to seismic action in the eurocode 8 of next generation. In: Vacareanu Radu, Ionescu Constantin (eds) *Progresses in European Earthquake Engineering and Seismology: Third European Conference on Earthquake Engineering and Seismology – Bucharest, 2022*. Springer International Publishing, Cham, pp 26–46. [https://doi.org/10.1007/978-3-031-15104-0\\_2](https://doi.org/10.1007/978-3-031-15104-0_2)
- Martins Luís, Silva Vítor, Bazzurro Paolo, Marques Mário (2018) Advances in the derivation of fragility functions for the development of risk-targeted hazard maps. *Eng Struct* 173:669–680. <https://doi.org/10.1016/j.engstruct.2018.07.028>
- Mayne P, Rix G (1995) Correlations between shear wave velocity and cone tip resistance in clays. *Soils Found* 35(2):107–110
- Meletti C, Marzocchi W, D'amico V, Lanzano G, Luzi L, Martinelli F, Pace B, Rovida A, Taroni M, Visini F, Akinci A, Anzidei M, Avallone A, Azzaro R, Barani S, Barberi G, Barreca G, Basili R, Bird P, Seno S (2021) The new Italian seismic hazard model (MPS19). *Ann Geophys*. <https://doi.org/10.4401/ag-8579>
- Pagani M, Monelli D, Weatherill G, Danciu L, Crowley H, Silva V, Henshaw P, Butler L, Nastasi M, Panzeri L, Simionato M, Vigano D (2014) OpenQuake engine: an open hazard (and risk) software for the global earthquake model. *Seismol Res Lett* 85(3):692–702
- Petersen MD, Shumway AM, Powers PM, Mueller CS, Moschetti MP, Frankel AD, Rezaeian S, McNamara DE, Luco N, Boyd OS, Rukstales KS, Jaiswal KS, Thompson EM, Hoover SM, Clayton BS, Field EH, Zeng Y (2020) The 2018 update of the US national seismic hazard model: overview of model and implications. *Earthq Spectra* 36(1):5–41. <https://doi.org/10.1177/8755293019878199>
- Pitolakis K, Gazepis C, Anastasiadis A (2006) Design response spectra and soil classification for seismic code provisions. In: *Proceedings of the ETC-12 workshop on geotechnical evaluation and application of the seismic Eurocode EC8 2003–2006*, 37–52
- Pitolakis K, Riga E, Anastasiadis A (2013) New code site classification, amplification factors and normalized response spectra based on a worldwide ground-motion database *Bull. Earthq Eng* 11(2013):925–966. <https://doi.org/10.1007/s10518-013-9429-4>
- Pitolakis K, Riga E, Anastasiadis A, Fotopoulou S, Karafagka S (2019) Towards the revision of EC8: proposal for an alternative site classification scheme and associated intensity dependent amplification factors. *Soil Dynam Earthq Eng*. <https://doi.org/10.1016/j.soildyn.2018.03.030>
- Pitolakis K, Riga E, Anastasiadis A (2020) Towards the revision of EC8: Proposal for an alternative site classification scheme and associated intensity-dependent amplification factors. In: *17th World Conference on Earthquake Engineering*, Sendai, Japan 13–18 Sep 2020.
- prEN 1998–1–1:2022 (2022) Eurocode 8: Earthquake resistance design of structures—Part 1: General rules and seismic action, Draft January 2022, European Committee for Standardization, Brussels, Belgium

- Riga E, Apostolaki S, Karatzetzou A, Laurentiu D, Pitilakis K (2022) The role of modelling of site conditions and amplification in seismic hazard and risk assessment at urban scale. The case of Thessaloniki, Greece. *Ital J Geosci* 141(2):198–215. <https://doi.org/10.3301/IJG.2022.16>
- Rovida A, Antonucci A (2021) EPICA-European PreInstrumental Earthquake CAtalogue, version 1.1. Istituto Nazionale di Geofisica e Vulcanologia (INGV). Dataset, <https://doi.org/10.13127/epica.1.1>
- Silva V, Crowley H, Pagani M, Monelli D, Pinho R (2014) Development of the openquake engine, the global earthquake model's open-source software for seismic risk assessment. *Nat Hazards* 72(3):1409–1427
- Silva V, Crowley H, Varum H, Pinho R (2015) Seismic risk assessment for mainland Portugal. *Bull Earthq Eng* 13:429–457. <https://doi.org/10.1007/s10518-014-9630-0>
- Silva V, Amo-Oduro D, Calderon A, Dabbeek J, Despotaki V, Martins L, Rao A, Simionato M, Viganò D, Yepes-Estrada C, Acevedo A, Crowley H, Horspool N, Jaiswal K, Journeay M, Pittore M (2018) Global Earthquake Model (GEM) Seismic Risk Map (version 2018.1), doi: <https://doi.org/10.13117/GEM-GLOBAL-SEISMIC-RISK-MAP-2018>
- Silva V, Brzev S, Scawthorn C et al (2022) A building classification system for multi-hazard risk assessment. *Int J Disaster Risk Sci* 13:161–177. <https://doi.org/10.1007/s13753-022-00400-x>
- Wald DJ, Allen TI (2007) Topographic slope as a proxy for seismic site conditions and amplification. *Bull Seismol Soc Am* 97(5):1379–1395
- Weatherill G, Kotha SR, Cotton F (2020) A regionally-adaptable regionally adaptable “scaled backbone” ground motion logic tree for shallow seismicity in Europe: application to the 2020 European seismic hazard model. *Bull Earthq Eng* 18:5087–5117. <https://doi.org/10.1007/s10518-020-00899-9>
- Weatherill G, Cotton F (2020) A ground motion logic tree for seismic hazard analysis in the stable cratonic region of Europe: regionalisation, model selection and development of a scaled backbone approach. *Bull Earthq Eng* 18:6119–6148. <https://doi.org/10.1007/s10518-020-00940-x>
- Weatherill GA, Crowley H, Roullé A, Tourlière B, Lemoine A, Gracianne Hidalgo C, Kotha SR, Cotton F, Dabbeek J (2021) European Site Response Model Datasets Viewer (v1.0). doi: <https://doi.org/10.7414/EUC-EUROPEAN-SITE-MODEL-DATA-VIEWER>
- Weatherill G, Crowley H, Roullé A, Tourlière B, Lemoine A, Gracianne C, Kotha SR, Cotton F (2022) Modelling site response at regional scale for the 2020 European Seismic Risk Model (ESRM20). *Bull Earthq Eng* 21:665–714
- Weatherill G, Kotha SR, Danciu L, Vilanova S, Cotton F (2023) Modelling seismic ground motion and its uncertainty in different tectonic contexts: Challenges and application to the 2020 European Seismic Hazard Model (ESHM20). *Nat. Hazards Earth Syst. Sci. Discuss.* [preprint], <https://doi.org/10.5194/nhess-2023-124>, in review
- Woessner J, Danciu L, Giardini D, Crowley H, Cotton F, Grünthal G, Valensise G, Arvidsson R, Basili R, Demircioglu MB, Hiemer S, Meletti C, Musson RMW, Rovida AN, Sesetyan K, Stucchi M (2015) The 2013 european seismic hazard model: key components and results. *Bull Earthq Eng* 13(12):3553–3596

**Publisher's Note** Springer Nature remains neutral with regard to jurisdictional claims in published maps and institutional affiliations.